

Review

# Toward Bactericidal Enhancement of Additively Manufactured Titanium Implants

Yingjing Fang<sup>1</sup>, Shokouh Attarilar<sup>2</sup> , Zhi Yang<sup>1</sup>, Guijiang Wei<sup>2,3</sup>, Yuanfei Fu<sup>1,\*</sup> and Liqiang Wang<sup>2,\*</sup>

<sup>1</sup> Shanghai Key Laboratory of Stomatology, National Center for Stomatology, National Clinical Research Center for Oral Diseases, Department of Prosthodontics, Shanghai Ninth People's Hospital, Shanghai Jiao Tong University School of Medicine; College of Stomatology, Shanghai Jiao Tong University, Shanghai 200011, China; fangyj1998@mail.sjtu.edu.cn (Y.F.); yangzhi412@alumni.sjtu.edu.cn (Z.Y.)

<sup>2</sup> State Key Laboratory of Metal Matrix Composites, School of Material Science and Engineering, Shanghai Jiao Tong University, Shanghai 200240, China; at.shokouh@gmail.com (S.A.); sjtuwgj@mail.sjtu.edu.cn (G.W.)

<sup>3</sup> Department of Medical Laboratory, Affiliated Hospital of Youjiang Medical University for Nationalities, Baise 533000, China

\* Correspondence: fuyf1421@sh9hospital.org.cn (Y.F.); wang\_liqiang@sjtu.edu.cn (L.W.)

**Abstract:** Implant-associated infections (IAIs) are among the most intractable and costly complications in implant surgery. They can lead to surgery failure, a high economic burden, and a decrease in patient quality of life. This manuscript is devoted to introducing current antimicrobial strategies for additively manufactured (AM) titanium (Ti) implants and fostering a better understanding in order to pave the way for potential modern high-throughput technologies. Most bactericidal strategies rely on implant structure design and surface modification. By means of rational structural design, the performance of AM Ti implants can be improved by maintaining a favorable balance between the mechanical, osteogenic, and antibacterial properties. This subject becomes even more important when working with complex geometries; therefore, it is necessary to select appropriate surface modification techniques, including both topological and chemical modification. Antibacterial active metal and antibiotic coatings are among the most commonly used chemical modifications in AM Ti implants. These surface modifications can successfully inhibit bacterial adhesion and biofilm formation, and bacterial apoptosis, leading to improved antibacterial properties. As a result of certain issues such as drug resistance and cytotoxicity, the development of novel and alternative antimicrobial strategies is urgently required. In this regard, the present review paper provides insights into the enhancement of bactericidal properties in AM Ti implants.

**Keywords:** additive manufacturing; porous titanium; implant coatings; antibacterial agent



**Citation:** Fang, Y.; Attarilar, S.; Yang, Z.; Wei, G.; Fu, Y.; Wang, L. Toward Bactericidal Enhancement of Additively Manufactured Titanium Implants. *Coatings* **2021**, *11*, 668. <https://doi.org/10.3390/coatings11060668>

Academic Editor: Grzegorz Dercz

Received: 8 April 2021

Accepted: 27 May 2021

Published: 31 May 2021

**Publisher's Note:** MDPI stays neutral with regard to jurisdictional claims in published maps and institutional affiliations.



**Copyright:** © 2021 by the authors. Licensee MDPI, Basel, Switzerland. This article is an open access article distributed under the terms and conditions of the Creative Commons Attribution (CC BY) license (<https://creativecommons.org/licenses/by/4.0/>).

## 1. Introduction

Bone infection is one the most serious and destructive risks associated with bone implant surgeries. According to the results of the International Consensus Meeting on Musculoskeletal Infection in 2018, the infection incidences for all orthopedic subspecialties ranged from 0.1% to 30%, and the cost of each patient ranged from USD 17,000 to 150,000 [1]. *Staphylococcus aureus* is considered to be the most common pathogen isolated from implant-associated osteomyelitis [2], and an increasing number of cases (more than 50%) are caused by refractory methicillin-resistant *S. aureus* (MRSA) strains [3]. Implants act as carriers for bacterial growth, increasing the bacterial virulence on the surface [4]. Bacteria adhere to the implant surface, before cell proliferation and biofilm formation [5]. A biofilm is a type of microbially derived fixation community that is characterized by cells that are irreversibly adhered to a substrate or interface between them, embedded in a matrix made up of their own extracellular polymeric substances [6]. Bacterial biofilms are resistant to antimicrobial treatments and evade host defenses by providing a physical barrier [7]. As a result of restricted blood flow, it is difficult to deliver antibiotics to the area around

the implant, and due to recurrence and drug resistance, the infection is often difficult to treat and will become chronic [8]. As a result, in these cases, the removal of the implant is sometimes necessary.

In recent years, various novel approaches have been proposed to prevent and treat implant-associated infections (IAIs). In order to endow titanium (Ti) implant surfaces with effective antimicrobial properties, two models were proposed: Passive antimicrobial mechanisms, which prevent the initial bacterial attachment, and active antimicrobial mechanisms, which release antimicrobial agents to kill adherent or planktonic bacteria. In addition, the local innate immune response should be enhanced, in order to stimulate immune cells to kill the bacteria [9]. Passive antimicrobial surfaces do not release antimicrobial agents; by changing the physicochemical properties of the surface, such as the roughness, hydrophilicity, or nanotopological structure, or by covalently immobilizing active molecules on the surface, they inhibit surface bacterial adhesion or kill bacteria by contact [10]. Active antimicrobial surfaces are loaded with antimicrobial agents through a variety of surface modification processes. They facilitate the controlled local release of antimicrobial agents that kill bacteria on the surface of the implant and around the tissue. Antibiotics [11], antibacterial active metals (such as silver (Ag) [12–14], copper (Cu) [15], zinc (Zn) [16]), and metal oxides [17] are widely applied in the study of implant antimicrobial surfaces. In a meta-analysis of 23 studies, Tsikopoulos et al. showed that a combination of active and passive antibacterial surfaces reduced the risk of IAIs [18].

Additive manufacturing (AM), often referred to as “3D printing”, enables the fabrication of scaffolds with high geometric complexity [19]. AM technology enables the fabrication of patient-tailored and structurally optimized porous implants through the precise design of external and internal structures [20–22]. Metal AM is composed of electron beam melting (EBM) [23,24], selective laser sintering (SLS) [25,26], selective laser melting (SLM) [27], laser engineered net shaping (LENS) [28,29], direct metal laser sintering (DMLS) [30,31], and laser aided AM methods [32]. Figure 1 shows several widely applied metal AM processes.

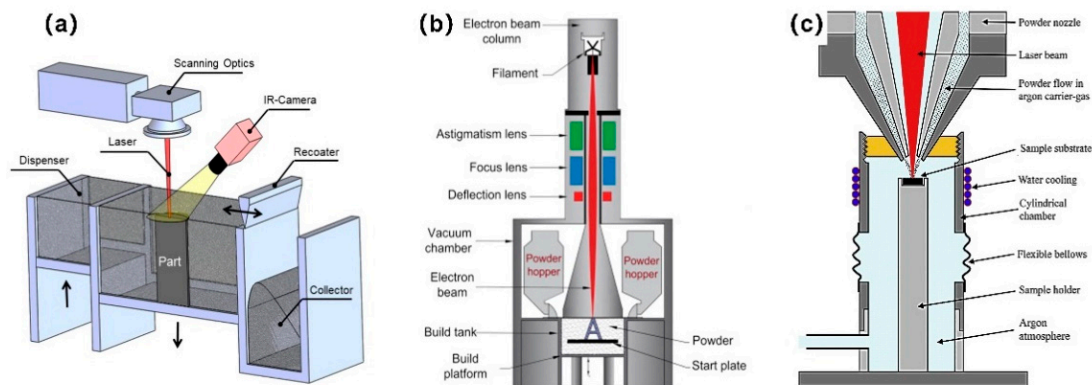


**Figure 1.** Schematic illustrations of the widely applied metal additive manufacturing (AM) processes: (a) Selective laser melting (SLM). Reprinted with permission from ref. [33]; (b) electron beam melting (EBM). Reprinted with permission from ref. [34]. Copyright 2017 Elsevier; (c) laser metal deposition (LMD). Reprinted with permission from ref. [35]. Copyright 2019 Elsevier.

At present, most implants in clinical use are bulk solid Ti with an elastic modulus much higher than that of bone, resulting in stress shielding [36]. The mechanical mismatch between the implant and the surrounding natural bone results in bone resorption [37]. AM technology enables the fabrication of patient-tailored and structurally optimized porous implants through the precise design of external and internal structures. Porous Ti implants have a suitable porosity and topological structure. This is achieved by mimicking the trabecular structure of natural bone tissue so that their mechanical properties match with the surrounding tissue, which can effectively transfer loads, reduce the stress shielding effect,

and promote osseointegration [38–40]. In addition, trabecular-like porous implants provide an open interconnecting space for cell growth and the transport of nutrient and metabolic waste. Osteoblasts and mesenchymal cells migrate and proliferate within the pores, which is accompanied by vascularization, facilitating bone ingrowth [41,42]. Although, at present, there is no consensus criteria, most studies show that improving porosity and pore size promotes bone tissue ingrowth into pores and the osseointegration of the implants on the basis of ensuring mechanical properties [41,43,44].

For metallic AM implants, a large number of studies focus on conferring antimicrobial properties through indirect means. For instance, the additional surface area of a porous or specially shaped AM implant is used to enhance the antimicrobial properties of surface biofunctionalized implants for protection against IAIs [45]. The same biofunctionalization treatments in in vitro tests showed that porous implants with an increased surface area release a significantly higher amount of antimicrobial agent and have an increased inhibition zone size as compared to solid implants with the same dimensions [46]. The difference is that for AM polymer implants, which are manufactured by fused deposition modeling (FDM) or stereolithography (SLA), antimicrobial agents such as antibiotics [47,48], quaternary ammonium salts [49,50], chitosan [51], and antimicrobial metal particles [52] are usually added to the raw material during the manufacturing stage to facilitate the generation of bactericidal surfaces. At present, there are very few studies on the direct preparation of antimicrobial Ti implants using AM. The following are various starting points from which to approach this: (1) Improving the AM processing parameters to obtain optimized surface physical properties and reduce bacterial adhesion [53]; (2) developing nano-AM technology to prepare nanoantibacterial structures on the implant surface [54]; (3) adding antimicrobial metal elements and exploring the appropriate proportion of elements to prepare the antimicrobial alloy using AM [55].

From another point of view, a porous structure is more conducive to bacterial growth than implants with smooth surfaces, and the increased surface area may also increase the number of bacteria that survive the disinfection process or cling to the surface before surgery [45]. There is, however, no clear evidence proving that porous implants have a higher incidence of IAIs than solid implants [56]. For example, trabecular metal implants are known as implants that have a porous structure. A great number of clinical trials compare the prognosis of trabecular metal implants and nontrabecular metal implants. Different clinical centers reported different revision rates for IAIs of the two types of implants, but the results were not statistically significant ( $p > 0.05$ ) [57–59]. It may be inferred that the increased surface area of AM porous implants has more effect on the antibacterial properties of the coating than the residual bacteria on the surface before surgery.

This review summarizes the various recently proposed strategies that improve the antibacterial properties of AM Ti implants. Firstly, the effect of AM technology on the antimicrobial properties of implants is discussed, and optimization schemes are proposed. Then, from the perspective of antimicrobial drug loading, drug release is explored through drug filling and implant surface bio-functionalization. Finally, the typical methods of antimicrobial functionalization of AM implants are listed, such as antibiotic coatings and antimicrobial active metal coatings.

## 2. The Effect of AM Technology on Antimicrobial Properties

An in vitro study found that Ti discs produced using the AM DMLS method could change the distribution of microbial species in subgingival biofilm and decrease the total counts of *Porphyromonas gingivalis*, which is the most widespread pathogen found in peri-implantitis [60]. Currently, AM processing parameters are being optimized and new AM technologies are being developed to improve antimicrobial performance.

Research shows that AM processing parameters were able to change the surface parameters and roughness of a Ti scaffold, such as the inclination angle, laser power, and beam diameter [61]. The inclination angle is a key design parameter, and it has been shown to be selective for the attachment of bacteria and tissue cells [53,62,63]. In the manufactur-

ing stage, by reducing the SLM build inclination angle, a lower biofilm-covered surface morphology can be constructed without changing the surface chemical properties of the scaffolds, which is characterized by a reduction in partially melted metal particles, leading to a decrease in the roughness and hydrophobicity (Figure 2) [53]. Villapún et al. [62] established a mathematical model to optimize the orientation of customized SLM implants, which can accurately predict and optimize the surface roughness of scaffolds. A case study focusing on the customized implant proved the feasibility of this method. The optimization of the inclination angle facilitates the rapid fabrication and functionalization of implants in a single-step process, without postprocessing or with only local processing. Ginestra et al. [64] found that the inclination angle has a limited effect on surface topography, highlighting the influence of different AM processing techniques on surface properties. It is not a simple task to explore the influence of a single parameter on antibacterial properties, and further in vitro and in vivo studies are required to this end.

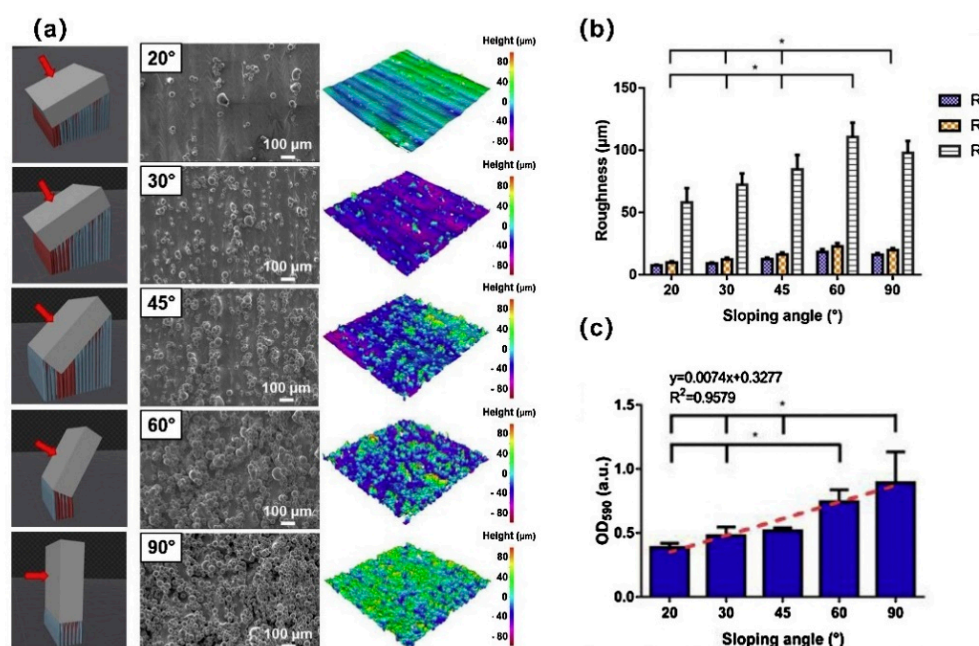


**Figure 2.** The SLM build inclination angle affects the surface roughness, which in turn affects bacterial adhesion. (a) Three-dimensional model of the build inclination angle, SEM micrograph images, and topographic scan of as-built Ti6Al4V samples with sloping angles from 20° to 90°; (b) measured arithmetic mean height ( $R_a$ ), root mean squared height ( $R_q$ ), and maximum height of profile ( $R_z$ ) as average values of 20 scans, where \* signifies  $p$ -value < 0.05 for  $R_a$ . (c) After 24 h of colonization, the biomass of *S. epidermidis* was quantified using crystal violet staining. Reprinted with permission from ref. [62]. Copyright 2020 Elsevier.

In the manufacturing process, the surface of the Ti implant inevitably retains some residual powders or partially melted particles. According to the report, it should be noted that this can inhibit the osteogenic activity of human bone marrow mesenchymal stem cells and enhance bacterial adhesion [65]. Therefore, AM scaffold surfaces are not suitable for direct use. Appropriate post-treatment care must be carried out before use [66]. The most common post-treatment methods include ultrasonic cleaning, sandblasting, chemical polishing, mechanical polishing, etc. The ability of ultrasonic cleaning to remove residual powder between the trabeculae on the surface is poor. In contrast, chemical polishing has a superior ability to remove powder residue and correlates with a decreased number of staphylococcal cells on the surface [67]. Junka et al. [68] speculated that fluoride and nitrogen on the surface of scaffolds could inhibit biofilm formation after chemical polishing. Sand blasting is a standard process for improving the surface finish in SLM production. However, it is worth noting that sandblasting may increase the risk of bacterial adhesion

on the implant surface if the sandblasting medium is not adequately removed [66,69]. Interestingly, Szymczyk-Ziolkowska et al. [70] found that different microorganisms have a species-specific ability to form biofilms on different types of implant modification. For patients with a history of *S. aureus*, *Pseudomonas aeruginosa*, or *Candida albicans* infection, the use of as-built, sandblasted, or acid-etched alloys are not recommended, respectively.

Metal AM technology is common and is processed on the microscale. For example, the surface arithmetic mean roughness ( $R_a$ ) of SLM is 5–20  $\mu\text{m}$  and the EBM is 20–50  $\mu\text{m}$  [71]. Several AM technologies with a nanoscale resolution have been developed, such as electron beam induced deposition (EBID) [72] and two-photon polymerization (TPP) [73]. TPP can produce 3D nanostructures and trigger the polymerization process by applying laser pulses on photosensitive materials. This is a 3D prototype technology for precisely controllable sub-100 nm AM structures [73,74]. EBID uses a focused electron beam to decompose the precursor molecules into two parts: The volatile part is desorbed and discharged, and the nonvolatile part is left on the substrate to form a nanosized deposition layer [75–77]. These nanoscale AM technologies are expected to produce specific nanotopographies to kill bacteria by, for example, inducing excessive levels of strain through a mechanical process [45]. Ganjian et al. [54] used EBID to fabricate nanopillars with precisely controlled dimensions within the osteogenic range on silicon wafers (Figure 3). To the authors' knowledge, nanoscale AM technology has not been applied to Ti implants, and the printing of antimicrobial nanopatterns on Ti implants requires further exploration.

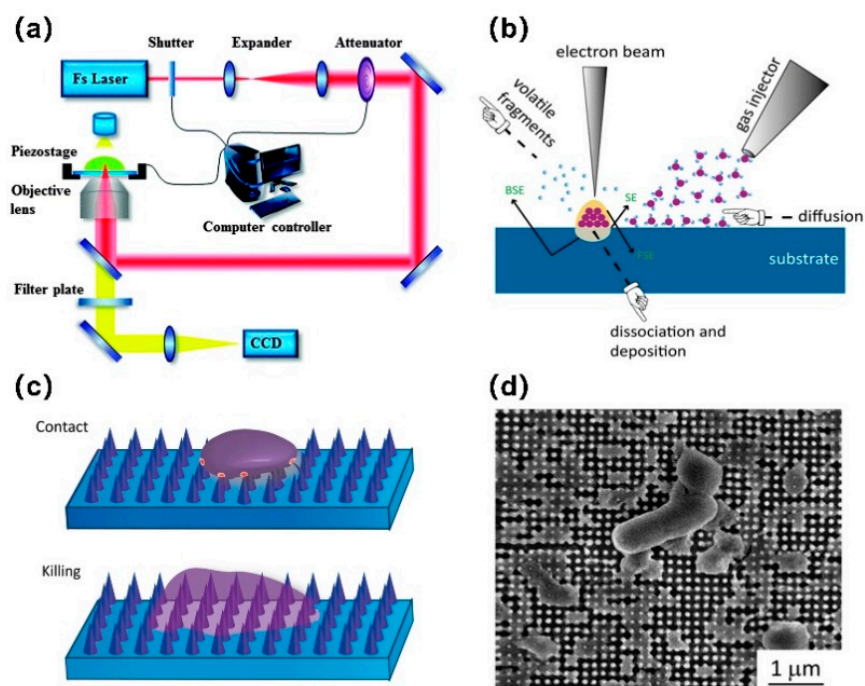


**Figure 3.** Schematic representation of (a) two-photon polymerization (TPP) (Reprinted with permission from ref. [78]. Copyright 2015 Royal Society of Chemistry) and (b) electron beam induced deposition (EBID); (c) schematic diagram showing the bactericidal behavior of a nanopattern structure, including deformation and being sunk on the nanopattern due to the penetration of the nanocolumn into the bacterial cell wall; (d) SEM image of damaged *Escherichia coli* bacteria on the surface of a nanopattern after 18 h of culture, observed from the above [54]. (CCD: Charge-coupled device).

### 3. AM Implants with Antimicrobial Loading

Oral or intravenous drug administration in the treatment of IAIs does not often work very well. This is due to the concentration of the drug in the blood, which is affected by the peak-and-valley effect. Additionally, drug release kinetics are often unpredictable, sometimes reaching toxic levels and sometimes falling below the therapeutic level. Moreover,

inadequate blood perfusion restricts the blood supply in the bones, and only very small quantities of the drug reach the target site. Under these circumstances, utilizing the implant as a loader of the local drug delivery system is a promising method: It facilitates controlled and sustained release, a high local drug concentration, and minimizes the treatment period required [79,80]. Current implant drug loading methods generally include drug filling through implant design, a surface coating that releases drugs, and drug reservoirs through surface modification [81].

### 3.1. Hollow Implants

Ti implants with void volumes were designed to be filled with antimicrobial agents. These are known as hollow implants. The geometric freedom of AM technology facilitates the manufacturing of complex internal structures that would not be achievable with traditional methods. Park et al. [82] implanted hollow Ti implants perforated with microholes and loaded with a dexamethasone-based cartridge into the tibia of rabbits. The plasma pharmacokinetic behavior in these samples showed that the agent could be released continuously up to 7 weeks after implantation. Furthermore, a stainless-steel porous-wall hollow implant designed by Gimeno et al. [83] was filled with the synthetic antibiotic linezolid and was shown to exhibit good anti-infection properties in a model of tibia infection in sheep. It seems that drug-filled hollow implants may represent a novel approach to treat or prevent IAs that do not require repeated injections or timely oral administration to maintain critical drug concentrations.

For the design of drug release routes, using microchannels for hollow implants is a typical method. The release profile can be pre-designed by selecting the number of channels in order to achieve a rapid initial release and a slow, sustained, long-term release [84]. With the assistance of AM technology, hollow Ti implants with different channel orientations can be manufactured. It was found that channel orientation can affect the accuracy of the channel dimension [85,86], the back-pressure porosity of the injection material, the drug elution rate, and even the direction of drug release (Figure 4) [85]. Bezuidenhout et al. [87] designed a Ti alloy cube with channels. Polyethersulfone membrane discs were placed at the opening of each channel. It was able to control the release rate for the drug, and repeatable filling with antibiotics was possible through polyethersulfone membranes. Thus, antibiotic levels could be maintained above the minimum inhibitory concentration (MIC) for an extended period and drug resistance could be avoided. AM technology can also provide thin permeable walls with different porosities for hollow Ti implants. With the increase in porosity, the pattern of drug release profiles changes [88].

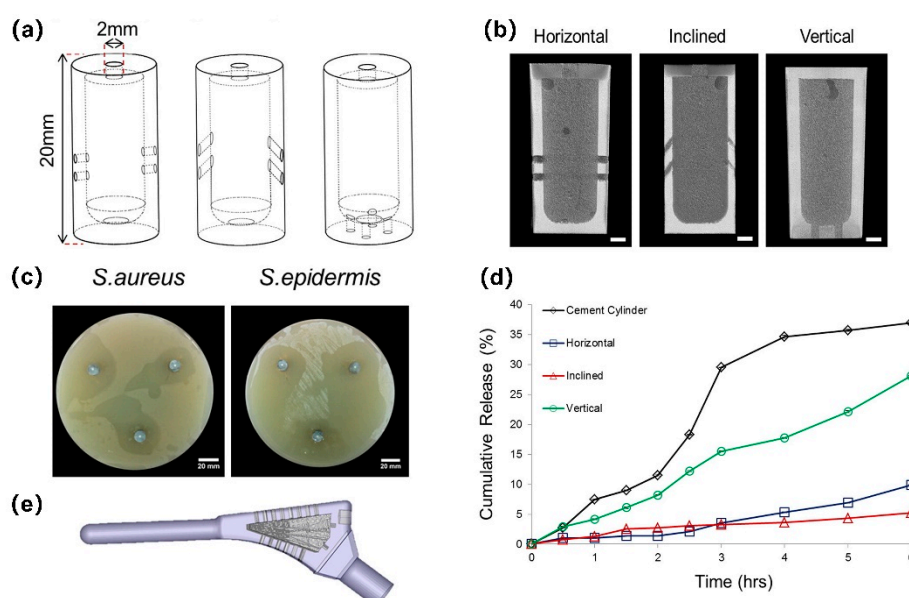


Figure 4. SLM Ti6Al4V implants containing a reservoir. Adapted with permission from ref. [85]. Copyright 2016 Elsevier.

(a) Schematics of implants with horizontal, inclined, and vertical pore channels; (b) coronal slice of antibiotic-loaded cement within implants; (c) zones of bacterial inhibition around implants with horizontally orientated pore channels showing directionality; (d) cumulative release of antibiotic from cement cylinders and cement-filled implants with different pore orientations; (e) re-engineered functional implant.

The filling material plays a pivotal role in the release spectrum, and its material type and solubility affect the reaction; for example, drugs with a higher water solubility exhibit a faster drug release rate [84]. The second factor is the state of the material that is filled. If the drug is directly filled, the elution involves one stage, and the drug is directly released from the channel. If the medium contains antibiotics, such as mesoporous silica particles or bone cement, the elution involves two stages: The drug is first desorbed from the medium and then released through the implant channels [85,89]. This two-stage eluting device has the ability to precisely control the drug release rate, because the drug medium and the hollow implant channel can be controlled independently.

The drug loading and drug eluting of these hollow Ti implants had promising antibacterial effects [85,88,90], which indicates that an optimized drug release profile could be achieved by rational structural design; however, a complete design scheme has not been proposed to date.

### 3.2. Porous Implants

#### 3.2.1. Bioactive Coating

As a result of the increased surface area of porous implants, there is great potential for loading antimicrobial agents through coatings and surface treatments. Burton et al. [91] studied eight unit cell types of AM porous lattices and determined that the original Schwartz lattice geometry with 10% volume filling maintains the loading capacity, while allowing the maximum void volume in all lattice designs to load more antimicrobial agents. In addition to a homogeneous porous lattice structure, AM technology can also be used to manufacture implants with gradient porosity or surface blind pores. Sukhorukova et al. [92] used SLS to prepare a square blind holes network structure for loading antibiotics onto the surface of Ti plates. This had an obvious antibacterial effect, which was superior to the standard plate that contained a higher concentration of antibiotics.

Active coatings release preincorporated antimicrobial agents, such as antibiotics [93], inorganic antimicrobials [94,95] (e.g., silver (Ag), zinc (Zn), copper (Cu), gallium (Ga)), antiseptics [96], antimicrobial peptides [97], or certain types of metal oxides, to downregulate infection [45,98]. The biocompatibility of the implants should be ensured while considering the antimicrobial properties. Inspired by the extracellular matrix and proteins, organic and inorganic (hydroxyapatite) components, and composition combinations of living bone tissue, many bioactive materials can be used as candidates for antibacterial agents to coat implant surfaces [99]. Such coatings are not only effective in loading antimicrobial agents, but they also have the potential to promote tissue integration. These coatings include durable/biodegradable polymers, nanofibers, hydroxyapatite and gels [81], and titania nanotubes (TNT), which can mimic the nanoscale topology of bone and are among the most promising implant coatings. When antibacterial agents are mixed with these bioactive materials, the final drug release from the AM porous Ti implant surface is determined by the complex interaction between the coating characteristics, the drug properties, and the in vivo conditions [100].

There are many emerging surface treatment methods. During surface treatment and the coating of porous Ti implants, it is key to form a uniform surface over the entire specimen, reaching the entire inner surface. Some traditional coating techniques, such as plasma spraying, result in poor control over the thickness and surface topography and are not suitable for porous implants with complex geometries [99]. Therefore, chemical or electrochemical technology is a better choice, in order to reach the inner surface of the porous structure [45,101]. Technologies such as dipping, biomimetic deposition, chemical

surface treatment using acidic and alkaline solutions, anodic oxidation, electrophoretic deposition, and plasma electrolytic oxidation are widely used in this field [45,99,102].

### 3.2.2. Nanometer Coating

In general, the nanomorphology of Ti surfaces with an antibacterial function is usually designed as nanotube and nanocoating forms [103]. TNT is easily adapted to AM porous structures and can be prepared on three-dimensional nonplanar surfaces [104]. A uniform layer of TNT can be formed on porous implants by liquid phase electrochemical treatment, e.g., anodizing [105,106] and micro-arc oxidation (MAO) [107–109]. In addition to the macroporous structure of AM technology, the microstructure of partially melted Ti microspheres on the surface of AM implants and TNT together constitutes a unique dual micro- to nanotopography (Figure 5) [110–112]. Biocompatibility and good corrosion resistance were demonstrated in TNT-coated Ti implants [113], and various promising results were reported in terms of improving the osteogenic activity around implants [111,114,115], especially regarding the dual micro- to nanotopography of AM porous scaffolds [111,116]. The hydrophilic surface of TNT has a positive effect on reducing bacterial adhesion, but the antibacterial performance of TNT is still poorer than that of mechanically polished samples, because the roughness of TNT affects its antibacterial properties [105].

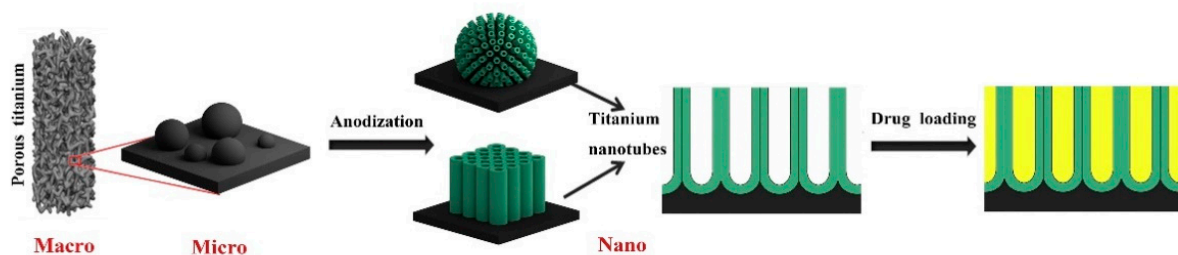


**Figure 5.** AM Ti implants with unique micro- and nanotopography, which can be used as a nano drug delivery system by combining AM technology and anodization. Adapted with permission from ref. [116]. Copyright 2020 Elsevier.

Nanotube structures with highly specific surface areas and pore volumes are both well organized and controllable and represent a good strategy for drug delivery and antibacterial activity [117]. Drug-eluting nanotubes significantly reduced bacterial adhesion to the surface when researchers filled the nanotubes with the antibiotic gentamicin [115]. Moreover, various parameters involved in anodizing (such as pore size and length) can precisely control the size of nanotubes [118], which, in turn, can control the drug release rate [119]. Drug-loaded TNT can be combined with other functional coatings, such as polymers [120] and hydrogels [116], which cover the openings of the TNTs and prolong the drug release time [121]. Maher et al. [122] proposed an innovative antimicrobial surface preparation method using SLM technology and electrochemical anodization to prepare the surfaces nanotopography of Ti alloys, thus promoting the nucleation reaction and growth of sharp nanospines through the hydrothermal process. The sharp triangular-shaped nanospines effectively destroyed bacteria by mechanically damaging their cell walls.

The majority of the research on nanocoatings focuses on metal nanoparticles [46,106,109] and nanocarriers, which aim to deliver antibacterial agents [123,124]. Metal nanoparticles have excellent antimicrobial effects [125]. Nanocoatings that do not contain antimicrobial agents are gradually being developed. Hu et al. [105] found that the composite effect of TNT and nanophase CaP on SLM Ti surfaces also exhibited good antibacterial activity. Furthermore, these antibacterial properties mainly come from the surface nanoroughness [105,123,126]. Rifai et al. [127] demonstrated that a nanodiamond (ND) coating can improve interface properties to inhibit bacterial colonization, and NDs coatings were applied on SLM Ti scaffolds using dip coating technology. Interestingly, it was found that controlling the embeddedness of nanoparticles is very helpful for maintaining the cell

adhesion and osteogenic differentiation potential of TNT, especially when the nanoparticles do not completely cover the nanotubes [123].

#### 4. Application of Antimicrobial Functionalization of AM Implants

##### 4.1. Antibiotic

Antibiotics are the standard clinical tool for the local and systemic treatment of various infections caused by broad-spectrum pathogens. The concentration of local antibiotics is much higher than that achieved through parenteral administration. It can even be delivered to nonvascular areas, which can reduce the risk of antibiotic resistance and systemic toxicity [128,129]. Antibiotic implant materials, such as bone cement and temporary bone cement spacers, have exhibited effective antibacterial activity. AM porous Ti implants provide a variety of strategies for local antibiotic administration, among which surface coating technology is the most widely studied. In addition, from the perspective of implant structure design, antibiotic-added reservoirs are an important emerging method (see Section 3.1).

AM porous Ti implants have inherent advantages, such as their high porosity and large surface area, which provide adhesion sites for antibiotics. Moreover, they can be loaded with more antibiotics. Griseti et al. [129] found that the antibacterial effect of 3D porous Ti loaded with antibiotics lasted for 7 days, which was similar to that of early antibiotic bone cement. Smooth Ti alloy beads loaded with antibiotics demonstrated a limited inhibition effect before the second day. The change in the surface topology also improved the release profile of antibiotics and significantly increased the release amount [107,123].

There are several factors that need to be considered when choosing the type of antibiotic. The first is the antibacterial spectrum of the antibiotics, followed by its compatibility with the coating processing technology, and its stability and solubility, which determine the release profile. Gentamicin and vancomycin are the most widely used antibiotics for the prevention and treatment of IAIs. They are active against both Gram-negative and Gram-positive bacteria. Gentamicin and tobramycin, which have broad-spectrum antimicrobial properties and high temperature resistance, were approved by the United States Food and Drug Administration (FDA) for incorporation into bone cement for the treatment of prosthetic joint infections [130]. Vancomycin belongs to the glycopeptide antibiotics family and is effective against MRSA [131]. With the increase in bacterial resistance, and even the emergence of vancomycin-resistant strains [132], there is an urgent need for the application of novel antibiotics or combinations of antibiotics to treat refractory IAIs. Molina-Manso et al. tested the drug susceptibility of staphylococcal biofilms with a variety of antibiotics and found that rifampicin and tigecycline exhibited superior anti-biofilm activity to other antibiotics, which could be applied on the surface of implants to treat or prevent IAIs [133]. In addition, daptomycin [134,135] and minocycline [136] demonstrated efficacy against MRSA biofilms [137].

Current studies on antibiotic coatings focus on optimizing the release kinetics of eluting antibiotics. One important consideration is the duration of drug release, which must take into account both early and delayed IAIs. Another is the concentration of the released drug, which can help to avoid the development of bacterial resistance. In general, the release of antibiotics can be divided as follows: There is an initial outbreak period, during which the drug concentration reaches a high level; then, the release continues above MIC and stops before the development of antibiotic resistance (Figure 6). Stigter et al. [138] used the biomimetic coprecipitation method to incorporate antibiotics into the HA coating of titanium implants. Among the eight antibiotics studied, cephalosporins containing carboxylic groups were more strongly bound to the coating, with higher incorporation, a slower release rate, and more durable and effective antimicrobial activity.

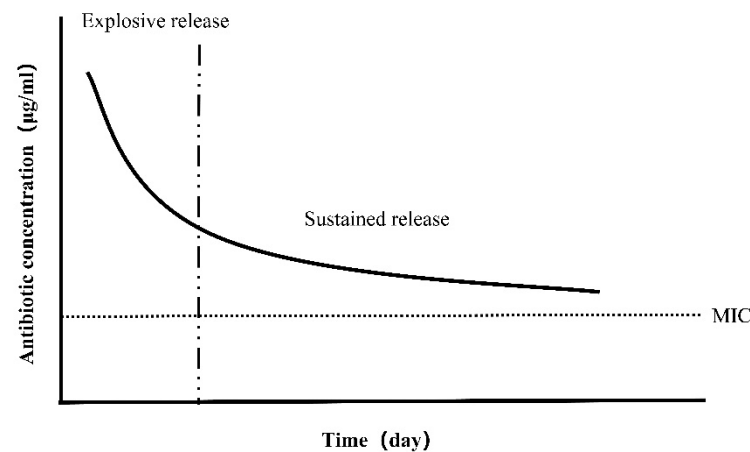


**Figure 6.** Ideal antibiotic release profile. The initial explosive release can kill bacteria effectively, and then the sustained release above the minimum inhibitory concentration (MIC) can maintain the antibacterial effect for a long period without antibiotic resistance.

Researchers have explored a variety of biocompatible coatings that stabilize adhesion to the Ti scaffold and load antibiotics. Common examples include dopamine [107], chitosan [139], gelatin [140], hyaluronic acid [141], and a variety of organic polymers [123,142–144]. Yavari et al. [140] applied multiple layers of gelatin- and chitosan-based coatings containing vancomycin and verified that the coating was almost completely degraded after 8 weeks. This timely biodegradation ensures the release of high doses of antibiotics during the perioperative period, while minimizing the risk of antibiotic resistance caused by long-term exposure to sub-MIC doses of antibiotics. Ghimire et al. [145] found that chitosan-fixed Ti implants significantly increased the sensitivity of adherent bacteria to antibiotics. Various innovative coatings, such as silk fibroin [146], bacterial cellulose [147], and phase-transited lysozyme [141], have also been proposed. Drug release from this conventional coating is continuous regardless of the occurrence of IAIs. In recent years, intelligent antimicrobial coatings have gradually emerged [148]. When the implant is invaded by bacteria and IAIs occurs, it is stimulated by temperature [149], pH [150], and electrical signals [151] to release antibiotics. Thus, the unnecessary release of antimicrobial agents in the uninfected state is avoided, and the risk of bacterial resistance is minimized.

Various processing and assembly methods have been explored that need to be suitable for customized scaffolds with complex shapes to ensure the continuous release of antibiotics. These include electrophoretic deposition (EPD) [128,143,146], electrospray deposition [123], covalent binding, layer-by-layer self-assembly [124,152], and electrospinning [142]. The advantage of EPD is that it can simply add a variety of antibacterial agents (such as antibiotics and nanoparticles) into different hydrogels and control the thickness and uniformity of the coating [143]. Given the hydrophilicity of antibiotics, EPD is a good approach. Bakhshandeh et al. [128] prepared chitosan and gelatin coatings in this way, and the antibiotics could be continuously released at a concentration higher than MIC for 21 days, thus achieving a long-term and highly effective bacteriostatic effect. Jahanmard et al. [142] applied antibiotic-loaded poly( $\epsilon$ -caprolactone) (PCL) and poly(L-lactic acid-co-glycolic acid) (PLGA) nanofiber coatings to lattice Ti implants by means of electrospinning. In this approach, the combination of specific drug–polymer interactions with bi-layer structures is crucial to prolong the inhibitory drug concentration, and, for the first time, it was shown that the antibacterial effect can last more than 6 weeks, preventing the early and delayed onset of IAI (Figure 7). Layer-by-layer self-assembly technology has great advantages in the stable fixation and continuous release of antibiotics. The self-assembled membrane prepared by Vaithilingam et al. [152] released less than 60% of the drug after 6 weeks.

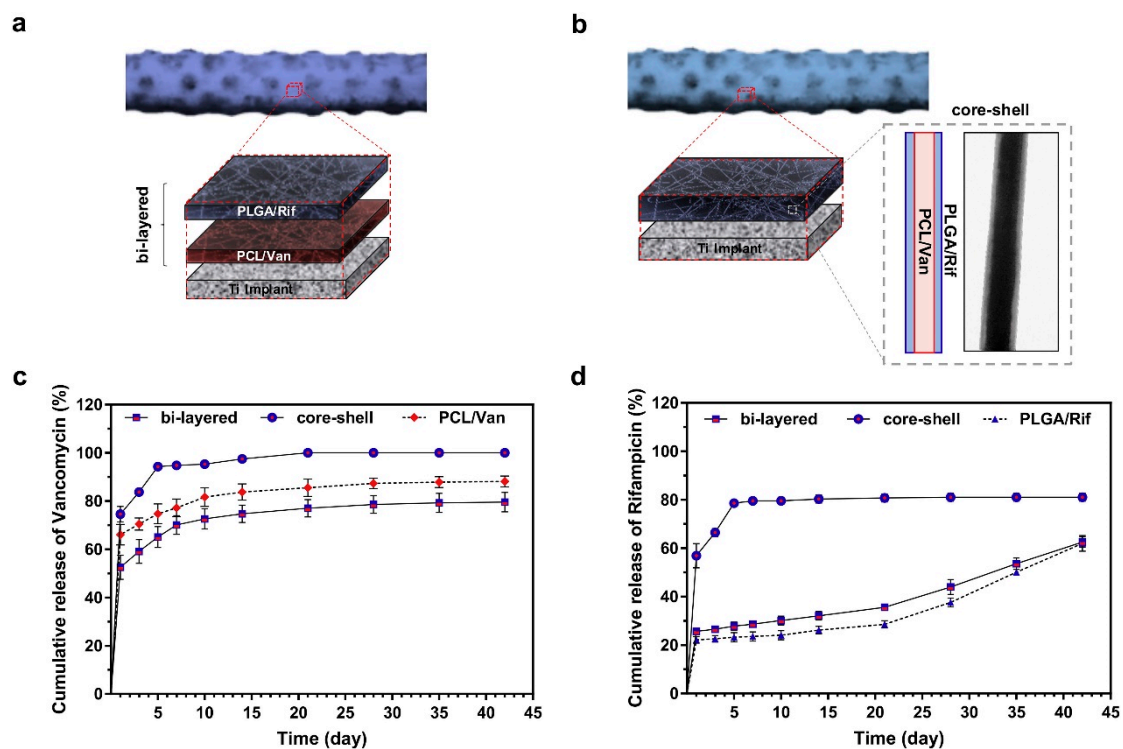


**Figure 7.** Various assembly and in vitro antibiotic release profiles of drug-loaded nanofiber-filled lattice implants. Reprinted with permission from ref. [142]. (a) The structure of the bi-layer nanofiber filled with PCL/Van as the inner layer and PLGA/Rif as the outer layer. (b) The structure of the core-shell nanofiber is composed of PCL/Van in the core and PLGA/Rif in the shell. The core-shell structure was verified by transmission electron microscope. Cumulative release of Van (c) and Rif (d) from three different nanofiber-filled lattice structures within 6 weeks. (Abbreviations: PCL, poly( $\epsilon$ -caprolactone); PLGA, poly(L-lactic-co-glycolic acid); Van, vancomycin; Rif, rifampicin.).

The traditional view is that antibiotics are not cytotoxicity, and most antibiotic coatings demonstrate good biocompatibility [128]; however, Sukhorukova et al. [139] found that a standard dose of gentamicin (40 mg/mL) had short-term toxicity at an early stage and inhibited the proliferation of osteoblasts. Because the strong antimicrobial activity due to early rapid drug release compromises biocompatibility, caution is needed when using high concentrations of antibiotics.

## 4.2. Antibacterial Active Metal

### 4.2.1. Silver

In order to improve the antibacterial properties of AM implants, Ag has been widely studied for its broad-spectrum antibacterial activity and low toxicity to mammalian cells [153]. Table 1 shows the antibacterial effect of the Ag coating prepared on AM implants by different methods.

The toxic effects of Ag on microorganisms are attributed to the production of Ag ions [154]. Ag ions produce three main mechanisms of antibacterial action [155]: (1) Ag<sup>+</sup>-induced direct membrane damage, through which Ag<sup>+</sup> can cause physical damage to the membrane and interact with sulfur-containing membrane proteins [156]; (2) through the reactive oxygen species (ROS) related to Ag<sup>+</sup>, wherein the concentration of ROS is not related to the form of Ag, but is mainly related to the final concentration of Ag<sup>+</sup> [157]; (3) the cells uptake Ag<sup>+</sup> as a result of membrane perforation, resulting in the interruption of ATP production and the inhibition of DNA replication [155]. Compared with Gram-positive bacteria, Ag<sup>+</sup> has faster, longer, and more effective bactericidal effects on Gram-negative bacteria [106,108,158]. This may be due to the existence of a thick peptidoglycan layer in *S. aureus*, which can inhibit the transport of Ag ions through the cell membrane and has a low

sensitivity [28]. Because of Ag's various antibacterial mechanisms, it is not easy to appear drug resistance, and it even has a strong antibacterial effect against MRSA [46].

To construct multifunctional porous implants, Ag ions are often combined with surface topological modification techniques to improve the osteogenic properties, as is the case for anodized TNT loaded with Ag [46,159]. Plasma electrolytic oxidation (PEO) can completely disperse and firmly adhere Ag nanoparticles (AgNPs) to the surface of the implant in a very short time by adding AgNPs into the electrolyte. AgNPs are encapsulated in an in-depth growth oxide layer to prevent the free circulation of AgNPs in the blood. The oxide layer causes AgNPs to become completely fixed, which can further prevent the potential nanotoxic effects [46]. Ag usually exists in the form of Ag<sub>2</sub>O in PEO coatings. Gao et al. prepared TNT arrays embedded with Ag<sub>2</sub>O nanoparticles on the surface of titanium using magnetron sputtering and anodic oxidation. Compared with the direct incorporation of Ag<sup>+</sup> into TNT, the Ag<sup>+</sup> release rate of Ag<sub>2</sub>O was slower and the biocompatibility was better [106]. In addition to surface topological modification, composite biological coatings such as multifunctional hydrogels [160], polydopamine [108], chitosan [139], calcium phosphate [126], or silk protein [161] can be used to further enhance the biocompatibility of implants. Devlin-Mullin et al. [162] coated the surface of SLM 3D Ti scaffolds with an Ag nanolayer using atomic layer deposition, which produced good antibacterial properties and biocompatibility in vitro and in vivo. It also promoted angiogenesis and osteogenesis after implantation in rat tibia.

It is very important to improve antibacterial effects and prolong the anti-infection time, as it takes a long time (3 months) to achieve normal osseointegration. AM porous scaffolds and surface topological modification increase the depth of the reservoir, thereby increasing the ability to immobilize antimicrobial agents [108]. On this basis, compared with simple solution soaking [163], electrodeposition [159] and polydopamine-assisted coating [108] can form an Ag coating with stronger adhesion properties, providing Ag ion release for longer, and enhancing biocompatibility and the antibacterial properties. Shivaram et al. [159] prepared Ag coatings using electrodeposition and reported the most persistent in vitro release of Ag<sup>+</sup> to date (27 weeks), with the release of Ag<sup>+</sup> being within the potential toxicity limit of cells of 10 ppm (g/mL). In vivo experiments at 12 weeks showed good osteointegration properties and biocompatibility, but the long-term antimicrobial effects were not reported. Polydopamine (PDA) is a mussel-inspired multifunctional material, which can be deposited in situ onto TiO<sub>2</sub> via covalent cohesion. It can also chelate and reduce noble metal ions, inhibit the oxidative dissolution of AgNPs, and facilitate the long-term sustained dynamic release of Ag<sup>+</sup>. In this way, the rigid TiO<sub>2</sub>/PDA/Ag coating can be easily constructed on Ti [164]. Jia et al. [108] achieved an ultra-high loading capacity and a sustained release of Ag<sup>+</sup> through Mao, PDA, and Ag deposition. The antibacterial activity of scaffolds against planktonic/adherent bacteria (Gram-negative and Gram-positive) and even existing biofilms lasted for 12 weeks.

The synergistic effects of Ag and antibiotics on biofilm destruction have been observed. For instance, Ag can enhance the antibacterial activity of antibiotics. As Ag ions increase bacterial membrane permeability (even at sublethal concentrations), drug-resistant bacteria become sensitive to antibiotics [165]. AgNPs can promote free Ag<sup>+</sup> and antibiotics to kill biofilm bacteria through degrading the main components (polysaccharides, proteins, and nucleic acids) of the biofilm [108,166]. The special combination of Ag and antibiotics slows the release of the two drugs and avoids an initial sudden release. Furthermore, the release rate of each bactericide depends on the presence of other antibacterial components, such as Ag ions and antibiotics. The eradication of planktonic bacteria and adherent bacteria confirmed the synergistic effect of Ag and antibiotics. Moreover, reducing the drug concentration is beneficial in order to avoid the toxicity from Ag ions or antibiotics [128,158]. The slow release of Ag<sup>+</sup> provides very good antibacterial protection after the depletion of the antibiotic reservoirs [158].

Many in vitro antibacterial studies show that Ag ions have good antibacterial activity against bacteria and biofilms; however, Ag ions are somewhat toxic to mammalian

cells, such as human mesenchymal stromal cells (hMSCs) [163], osteoblast-like cells [128], and macrophages [167]. The early explosion of Ag ions may lead to osteoblast toxicity; however, in the later stage, the toxicity is weakened when the Ag ion concentration is reduced, and the proliferation activity of osteoblasts is enhanced, which can offset the side effects in the early stage [108,161]. Two different outcomes were found when Ag-loaded chitosan-coated implants were implanted into the body. In the absence of infection or a low bacterial challenge, the host reaction can overcome the cytotoxicity of Ag, exhibiting a good antibacterial effect. When the host faces a high bacterial challenge, 0.1–1  $\mu\text{m}$  Ag particles trigger inflammation and are released from the implant surface, which mediates local over-inflammation; kills neutrophils, so there is no antibacterial effect; and even aggravates infection-mediated bone remodeling [139]. Therefore, further in vivo studies are needed before Ag-coated implants will be ready for clinical use.

**Table 1.** The antibacterial effect of Ag coating prepared on AM implants.

Implant	AM Technology	Microorganism	Coating Technology	Result	Duration	Reference
Ti6Al4V	SLM	MRSA	PEO using electrolytes based on Ca/P species and AgNPs	Release of Ag ions; In vitro, antibacterial behavior against MRSA; Ex vivo, murine femoral infection model	4 weeks; 24 h; NR	[46,168,169]
Ti6Al4V	EBM	<i>E. coli</i> and <i>S. aureus</i>	MAO and PDA/Ag treatments	In vitro, antibacterial behavior against <i>E. coli</i> and <i>S. aureus</i> both planktonic and in biofilm	12 weeks	[108]
Ti6Al4V	EBM	<i>S. aureus</i>	Electrophoretic deposition of Ag and calcium phosphate nanoparticle layers	In vitro, antibacterial behavior against <i>S. aureus</i>	17 h	[126]
Ti	SLS	<i>E. coli</i> , <i>S. aureus</i> and <i>N. crassa</i>	TiCaPCON-Ag films by magnetron sputtering and loaded with gentamicin and amphotericin B	In vitro, antibacterial behavior against <i>E. coli</i> , <i>S. aureus</i> and <i>N. crassa</i>	3 days	[158]
Ti	LENS	NA	Anodized TNT followed by electrodeposition of Ag	Release of Ag ions	27 weeks	[159]
Ti	DMP	<i>S. aureus</i>	AgNO <sub>3</sub> were mixed with chitosan followed by EPD	In vitro, antibacterial behavior against <i>S. aureus</i> ; In vivo, tibia intramedullary implant model inoculated with <i>S. aureus</i>	1 week; NR	[139]

Table 1. Cont.

Implant	AM Technology	Microorganism	Coating Technology	Result	Duration	Reference
Ti6Al4V	EBM	<i>S. aureus</i>	Hydrothermal growth of a titanate layer, on which nanosilver encapsulated silk fibrin multilayers were anchored through PDA-assisted, silk-on-silk self-assembly	In vitro, antibacterial activity against clinical pathogenic <i>S. aureus</i> both planktonic and in biofilm	6 weeks	[161]
Ti	SLM	<i>S. epidermidis</i> and MRSA	Atomic layer deposition of an Ag nanolayer	In vitro, antibacterial behavior against <i>S. epidermidis</i> and no antibacterial activity against MRSA; In vivo, vascularization and osseointegration tendency	4 days; NR	[162]
Ti	DMP	<i>S. aureus</i>	Anodized TNT followed by soaking in AgNO <sub>3</sub> solution	In vitro, antibacterial behavior against <i>S. aureus</i>	2 weeks	[163]
Ti	DMP	<i>S. aureus</i>	Vancomycin and AgNO <sub>3</sub> were mixed with the Chitosan/gelatin compound followed by EPD	In vitro, antibacterial behavior against <i>S. aureus</i> both planktonic and in biofilm	3 weeks	[128]

Abbreviations: SLM, selective laser melting; EBM, electron beam melting; SLS, selective laser sintering; LENS, laser engineered net shaping; DMP, direct metal printing; MRSA, methicillin-resistant *S. aureus*; PEO, plasma electrolytic oxidation; MAO, micro-arc oxidation; EPD, electrophoretic deposition; AgNPs, Ag nanoparticles; PDA, polydopamine; TNT, titania nanotubes; NR, never report.

#### 4.2.2. Copper

Cu is a potential broad-spectrum inorganic antimicrobial agent. It is a necessary trace element in the human body and participates in the synthesis of enzymes. Cu is less cytotoxic than Ag [170] and can be metabolized by the human body. Therefore, Cu may be an effective substitute for Ag. It not only exhibits antibacterial activity against *E. coli* and *S. aureus* [171], but also demonstrates antibacterial and antibiofilm properties against the oral-specific bacteria *Streptococcus mutans* and *Porphyromonas gingivalis* [172], which is beneficial for using in dental materials. However, high doses of Cu can cause cytotoxicity. It is important to find the optimal concentration of Cu ions that can inhibit bacterial growth while avoiding cytotoxicity. Fowler et al. [173] studied the effect of Cu on the viability of

MC3T3 cells and *Staphylococcus epidermidis* in vitro, and the minimum inhibitory concentration of Cu ions in these two species ranged from  $9 \times 10^{-5}$  to  $9 \times 10^{-6}$  g/mL. As a result of species-specific and in vivo and in vitro differences, further studies are needed. At appropriate concentrations, Cu-modified implants also exhibited anti-inflammatory, proangiogenic, and osteogenic effects [174].

The antimicrobial mechanism of Cu can be divided into two elements: The direct mechanism and the indirect mechanism. The direct bactericidal mechanism involves Cu ions interacting with bacteria or biofilms. A large number of Cu ions flow into the bacteria, blocking the cell respiration chain and disturbing DNA synthesis. Then, a large amount of ROS are produced, leading to changes in the permeability of bacterial cell walls and leakage of the bacterial contents [175]. Cu inhibits the expression and transcription of positive biofilm regulators such as *sae* and *agr*, which inhibits biofilm formation [176]. The indirect bactericidal mechanism involves Cu activating the bactericidal ability mediated by macrophages. Cu can improve the ability of macrophages to uptake and kill bacteria, and it kills bacteria through the ROS pathway [177]. The concentration of copper ions required for the activation of macrophages is far lower than that required by the direct bactericidal mechanism, which can effectively help to avoid the cytotoxicity caused by high concentrations.

Similar to the method used for the preparation of the Ag coating, ion implantation [178], PEO [16], sol-gel [179], and electrodeposition [180] are applied in the preparation of copper coatings. For AM implants with complex geometries, PEO [16] and electrochemically assisted deposition [180] seem to be the superior methods. Interestingly, the application of copper as an antibacterial active substance in implants is not only through surface modification; copper-containing titanium alloy has also received much interest from researchers [181–183]. In the additive manufacturing process, Cu is added into the material by in situ alloying; thus, the process flow is simplified to a single-step process. In addition, it can help to avoid the wear and tear associated with surface coating and is expected to provide a lasting antibacterial effect. The antimicrobial properties of AM copper-containing titanium alloy are related to the Cu content, AM processing parameters, and heat treatment [181,183,184]. The majority of researchers consider 5 wt.% Cu to be appropriate for antibacterial function [184]. Furthermore, the in situ alloying of Cu increases the hardness and compressive strength of the material [185], which maintains good corrosion resistance in simulated body fluids [184].

In the preparation process, the phase transformation of antibacterial active metals inevitably occurs, such as during electrochemical treatments or powder processing at high temperatures, which may lead to the oxidation of the metal. Shimabukuro et al. [186] embedded Cu in the TiO<sub>2</sub> layer on the implant surface using MAO. They found that Cu existed in the form of Cu<sub>2</sub>O and exerted an antibacterial effect. Therefore, it is necessary to further explore the antibacterial effects of metal oxides. The oxides of Cu are Cu<sub>2</sub>O and CuO. Zhao et al. mixed Cu<sub>2</sub>O nanoparticles of different concentrations into the ceramic oxide layer using MAO. They found that the addition of Cu<sub>2</sub>O improved the antimicrobial performance of the MAO coating in a dose-dependent manner. It has also been demonstrated that Cu<sup>+</sup> is the key factor in terms of the antibacterial properties [187]. By comparing the minimum inhibitory concentrations and minimum bactericidal concentrations of Cu<sub>2</sub>O and CuO against four kinds of periimplantitis-related bacteria, it can be inferred that Cu<sub>2</sub>O has a superior antibacterial activity to CuO [17].

#### 4.2.3. Zinc

Compared with Ag, Zn has been less studied as an antimicrobial active substance, but its interesting biological effects have been gradually attracting attention. Zn is an essential trace element in the human body, which is involved in a variety of physiological processes, such as bone metabolism, cell signaling pathways, and immune regulation. Zn regulates the expression of bone morphogenetic protein gene, increases the activity of alkaline phosphatase, inhibits the bone resorption of osteoclasts, and induces the differentiation of

osteoblasts, thus promoting bone formation. In addition, Zn ions and their nanoparticles have good antibacterial properties. Zn ions (positive charge) and the cell wall of bacteria (negative charge) are attracted to each other by electrostatic interaction, resulting in the destruction of the bacteria cell wall. Moreover, Zn ions enter the bacteria and interfere with DNA replication [188]. Not only does Zn itself have the ability to kill bacteria directly, but it can also inhibit bacterial infection by regulating host immune defenses [189]. Wang et al. prepared ZnO films on a titanium surface using magnetron sputtering. The results of the *in vivo* experiments demonstrated a stronger antibacterial effect than in the *in vitro* experiments, indicating that Zn further enhanced the antibacterial effect by regulating the immune system response *in vivo*.

Similar to Ag and Cu, electrochemical deposition [190], MAO [191], and layer-by-layer self-assembly [192] are used to introduce Zn onto the implant surface. Liu et al. [192] constructed a bio-multilayer structure containing Zn ions using the self-assembly technique, which promoted the biological activity and function of osteoblasts and produced antibacterial activity at the same time. Different from the inert surface of pure titanium, the Zn-containing surface has the ability to induce osteogenesis while avoiding IAs, which is a promising modification method for biological implants.

In the Zn-doped TiO<sub>2</sub> layer prepared using EPO, Zn mainly exists in the form of ZnO. Surprisingly, when the MAO coating containing Zn was immersed in normal saline, the chemical state of the surface Zn changed from Zn<sup>2+</sup> to ZnO, leading to an increase in antibacterial activity [191]. ZnO nanoparticles have attracted much attention because of their biocompatibility, low toxicity, chemical stability, antimicrobial activity, and their selective killing effect on normal cells and cancer cells. In particular, the small size effect of ZnO nanoparticles plays an important role in their antibacterial behavior, inhibiting the growth of a variety of bacteria [193,194].

#### 4.2.4. Other Metals

Other metals such as gold (Au) [194], magnesium (Mg) [195], iron (Fe) [196], and their oxides also exhibit antibacterial effects. Au has stable chemical properties, good biocompatibility, and has the potential to promote the proliferation and differentiation of mesenchymal stem cells [197]. In addition, gold nanorods have special photophysical properties, which produce photothermal effects under the excitation of near-infrared light and exhibit antibacterial activity against a variety of bacterial strains [198]. The superparamagnetism of iron oxide nanoparticles makes targeted drug delivery possible. Moreover, it enables iron oxide nanoparticles to target the biofilm in the infected site and have a strong killing effect on drug-resistant strains [196].

#### 4.2.5. Comparison

Ag, Cu, and Zn are the most commonly used inorganic antimicrobial agents. A comparison of their biological effects is necessary to improve their various applications. The MIC of Cu and Zn is much higher than that of Ag, with a difference of about two orders of magnitude. The antimicrobial activity of Ag is higher than that of Cu and Zn, i.e., Ag can produce a high level of antimicrobial activity at a lower concentration [16]. However, Ag is more likely to cause cytotoxicity, and its half maximal inhibitory concentration (IC<sub>50s</sub>) to osteoblasts MC3T3-E1 is only 2.77 μM, while Cu and Zn show good biocompatibility in the appropriate concentration range, with IC<sub>50s</sub> of 15.9 and 90.0 μM, respectively [199]. A combination of antimicrobial agents provides a way to solve these two problems. The combination of two or more antibacterial agents has a synergistic antibacterial effect and reduces the minimum inhibitory or bactericidal concentration [169,180,200]. For example, the combination of Ag and Zn can reduce the required concentration of Ag by two orders of magnitude, while maintaining the same antibacterial activity, greatly reducing cytotoxicity [169]. Strontium (Sr), a metal ion with osteogenic activity, was doped with Ag on the implant surface. It not only exhibited strong synergistic antibacterial behavior against drug-resistant strains, but also polarized macrophages (M2) through favorable

immune regulation, thus further promoting the differentiation of preosteoblasts [168,201]. Shimabukuro et al. also investigated the biodegradation behavior of antibacterial active metal surfaces and found that their antibacterial properties had a time transient effect. When the antibacterial surface was soaked in normal saline for 28 days, the chemical states of the antibacterial active elements changed separately, leading to completely different changes in the antibacterial activity. The antimicrobial activity of the silver-coated specimens was gradually weakened, and Cu showed no significant change, while Zn showed enhanced antimicrobial activity [170].

Finally, it is important to note that although these antimicrobial active metals have shown excellent antimicrobial efficacy, they have not been approved as antimicrobial active ingredients in implants by the Food and Drug Administration (FDA) and Environmental Protection Agency (EPA) due to their potential cytotoxicity. Extreme caution should be exercised in the clinical application of these metal active ingredients until *in vivo* safety is further determined.

## 5. Conclusions

AM technology is increasingly being applied in orthopedics and stomatology, and the significant production freedom enables various innovative designs that cannot be achieved by traditional manufacturing methods. Through AM topological design, the mechanical properties and osteogenic properties of implants have been greatly improved. However, further optimization is needed to produce clinical applications. It is necessary to apply the surface modification technology of traditional solid titanium implants to the post-treatment of AM implants. Kirmanidou et al. [202] summarized a variety of surface modification methods to improve the mechanical properties, osteogenic properties, and antibacterial properties of titanium implants. Whether these surface modification methods are suitable for AM implants depends on whether they can be uniformly treated on surfaces with complex geometrical shapes, such as anodizing, acid/alkali treatments, and other liquid environments, in which surface modification methods are suitable. Sandblasting does not produce uniform modification of internal and external surfaces and is not suitable for AM implants with complex geometrical shapes.

In order to ensure the service life and suitability of AM Ti implants, antibacterial activity is not inconsequential. In this paper, various recent antimicrobial strategies applied to AM Ti implants are reviewed; however, the design of structural and antimicrobial coatings based on AM Ti implants remains a long way off. In the future, a balance between mechanical properties [203], microstructures and cell response [204], osteogenic properties, and antibacterial properties should be pursued in structural design. For antibacterial coatings, the release kinetics of antibacterial drugs might be further improved to suppress drug resistance and reduce the immune response caused by coating wear. The direct manipulation of AM technology to produce surfaces with inherent antimicrobial properties on AM Ti implants is also extremely promising. On the one hand, the antibacterial strategies of traditional Ti implants should be further applied to AM Ti implants, with emphasis on the development of surface treatment technologies suitable for complex geometries. On the other hand, novel and alternative strategies should be sought to combat IAI, especially through the development of AM technology to improve antimicrobial performance and simplify the processing method. For the clinical application of these implants with bactericidal or bacteriostatic properties, and in order to improve the biocompatibility and prolong the functional life of implants, further research is needed. In particular, *in vivo* trials are necessary before clinical human trials can commence.

**Funding:** The work was funded by the National Natural Science Foundation of China (Grant No. 31971246).

**Institutional Review Board Statement:** Not applicable.

**Informed Consent Statement:** Not applicable.

**Data Availability Statement:** Not applicable.

**Acknowledgments:** We are very grateful to the National Natural Science Foundation of China (No. 31971246) Fund Committee for its support.

**Conflicts of Interest:** The authors declare no conflict of interest.

## References

- Schwarz, E.M.; Parvizi, J.; Gehrke, T.; Aiyer, A.; Battenberg, A.; Brown, S.A.; Callaghan, J.J.; Citak, M.; Egol, K.; Garrigues, G.E.; et al. 2018 International Consensus Meeting on Musculoskeletal Infection: Research Priorities from the General Assembly Questions. *J. Orthop. Res.* **2019**, *37*, 997–1006. [[CrossRef](#)]
- Pulido, L.; Ghanem, E.; Joshi, A.; Purtill, J.J.; Parvizi, J. Periprosthetic joint infection: The incidence, timing, and predisposing factors. *Clin. Orthop. Relat. Res.* **2008**, *466*, 1710–1715. [[CrossRef](#)]
- Kaplan, S.L. Recent lessons for the management of bone and joint infections. *J. Infect.* **2014**, *68* (Suppl. 1), S51–S56. [[CrossRef](#)] [[PubMed](#)]
- Gristina, A.G.; Naylor, P.; Myrvik, Q. Infections from biomaterials and implants: A race for the surface. *Med. Prog. Technol.* **1988**, *14*, 205–224.
- Ricciardi, B.F.; Muthukrishnan, G.; Masters, E.; Ninomiya, M.; Lee, C.C.; Schwarz, E.M. Staphylococcus aureus Evasion of Host Immunity in the Setting of Prosthetic Joint Infection: Biofilm and Beyond. *Curr. Rev. Musculoskelet. Med.* **2018**, *11*, 389–400. [[CrossRef](#)] [[PubMed](#)]
- Costerton, J.W.; Montanaro, L.; Arciola, C.R. Biofilm in implant infections: Its production and regulation. *Int. J. Artif. Organs* **2005**, *28*, 1062–1068. [[CrossRef](#)] [[PubMed](#)]
- Masters, E.A.; Trombetta, R.P.; de Mesy-Bentley, K.L.; Boyce, B.F.; Gill, A.L.; Gill, S.R.; Nishitani, K.; Ishikawa, M.; Morita, Y.; Ito, H.; et al. Evolving concepts in bone infection: Redefining “biofilm”, “acute vs. chronic osteomyelitis”, “the immune proteome” and “local antibiotic therapy”. *Bone Res.* **2019**, *7*, 20. [[CrossRef](#)] [[PubMed](#)]
- Bjarnsholt, T. The role of bacterial biofilms in chronic infections. *APMIS Suppl.* **2013**, 1–51. [[CrossRef](#)]
- Qin, S.; Xu, K.; Nie, B.; Ji, F.; Zhang, H. Approaches based on passive and active antibacterial coating on titanium to achieve antibacterial activity. *J. Biomed. Mater. Res. A* **2018**, *106*, 2531–2539. [[CrossRef](#)] [[PubMed](#)]
- Bekmurzayeva, A.; Duncanson, W.J.; Azevedo, H.S.; Kanayeva, D. Surface modification of stainless steel for biomedical applications: Revisiting a century-old material. *Mater. Sci. Eng. C* **2018**, *93*, 1073–1089. [[CrossRef](#)]
- Chouirfa, H.; Bouloussa, H.; Migonney, V.; Falentin-Daudré, C. Review of titanium surface modification techniques and coatings for antibacterial applications. *Acta Biomater.* **2019**, *83*, 37–54. [[CrossRef](#)]
- Sobolev, A.; Valkov, A.; Kossenko, A.; Wolicki, I.; Zinigrad, M.; Borodianskiy, K. Bioactive Coating on Ti Alloy with High Osseointegration and Antibacterial Ag Nanoparticles. *ACS Appl. Mater. Interfaces* **2019**, *11*, 39534–39544. [[CrossRef](#)]
- Xie, C.-M.; Lu, X.; Wang, K.-F.; Meng, F.-Z.; Jiang, O.; Zhang, H.-P.; Zhi, W.; Fang, L.-M. Silver Nanoparticles and Growth Factors Incorporated Hydroxyapatite Coatings on Metallic Implant Surfaces for Enhancement of Osteoinductivity and Antibacterial Properties. *ACS Appl. Mater. Interfaces* **2014**, *6*, 8580–8589. [[CrossRef](#)]
- Fazel, M.; Salimijazi, H.R.; Shamanian, M.; Minneboo, M.; Modaresifar, K.; van Hengel, I.A.J.; Fratila-Apachitei, L.E.; Apachitei, I.; Zadpoor, A.A. Osteogenic and antibacterial surfaces on additively manufactured porous Ti-6Al-4V implants: Combining silver nanoparticles with hydrothermally synthesized HA nanocrystals. *Mater. Sci. Eng. C Mater. Biol. Appl.* **2021**, *120*, 111745. [[CrossRef](#)]
- Jacobs, A.; Renaudin, G.; Forestier, C.; Nedelec, J.M.; Descamps, S. Biological properties of copper-doped biomaterials for orthopedic applications: A review of antibacterial, angiogenic and osteogenic aspects. *Acta Biomater.* **2020**, *117*, 21–39. [[CrossRef](#)]
- van Hengel, I.A.J.; Tierolf, M.; Fratila-Apachitei, L.E.; Apachitei, I.; Zadpoor, A.A. Antibacterial Titanium Implants Biofunctionalized by Plasma Electrolytic Oxidation with Silver, Zinc, and Copper: A Systematic Review. *Int. J. Mol. Sci.* **2021**, *22*, 3800. [[CrossRef](#)]
- Vargas-Reus, M.A.; Memarzadeh, K.; Huang, J.; Ren, G.G.; Allaker, R.P. Antimicrobial activity of nanoparticulate metal oxides against peri-implantitis pathogens. *Int. J. Antimicrob. Agents* **2012**, *40*, 135–139. [[CrossRef](#)] [[PubMed](#)]
- Tsikopoulos, K.; Sidiropoulos, K.; Kitridis, D.; Hassan, A.; Drago, L.; Mavrogenis, A.; McBride, D. Is coating of titanium implants effective at preventing *Staphylococcus aureus* infections? A meta-analysis of animal model studies. *Int. Orthop.* **2021**, *45*, 821–835. [[CrossRef](#)] [[PubMed](#)]
- Attarilar, S.; Ebrahimi, M.; Djavanroodi, F.; Fu, Y.; Wang, L.; Yang, J. 3D Printing Technologies in Metallic Implants: A Thematic Review on the Techniques and Procedures. *Int. J. Bioprint.* **2021**, *7*, 306. [[CrossRef](#)] [[PubMed](#)]
- Bose, S.; Traxel, K.D.; Vu, A.A.; Bandyopadhyay, A. Clinical significance of three-dimensional printed biomaterials and biomedical devices. *MRS Bull.* **2019**, *44*, 494–504. [[CrossRef](#)] [[PubMed](#)]
- Zheng, C.; Attarilar, S.; Li, K.; Wang, C.; Liu, J.; Wang, L.; Yang, J.; Tang, Y. 3D-printed HA15-loaded beta-Tricalcium Phosphate/Poly (Lactic-co-glycolic acid) Bone Tissue Scaffold Promotes Bone Regeneration in Rabbit Radial Defects. *Int. J. Bioprint.* **2021**, *7*, 317. [[CrossRef](#)]
- Maconachie, T.; Leary, M.; Lozanovski, B.; Zhang, X.Z.; Qian, M.; Faruque, O.; Brandt, M. SLM lattice structures: Properties, performance, applications and challenges. *Mater. Des.* **2019**, *183*, 18. [[CrossRef](#)]

23. Murr, L.E. Open-cellular metal implant design and fabrication for biomechanical compatibility with bone using electron beam melting. *J. Mech. Behav. Biomed. Mater.* **2017**, *76*, 164–177. [[CrossRef](#)] [[PubMed](#)]
24. Trevisan, F.; Calignano, F.; Aversa, A.; Marchese, G.; Lombardi, M.; Biamino, S.; Ugues, D.; Manfredi, D. Additive manufacturing of titanium alloys in the biomedical field: Processes, properties and applications. *J. Appl. Biomater. Funct. Mater.* **2018**, *16*, 57–67. [[CrossRef](#)] [[PubMed](#)]
25. Hafeez, N.; Liu, S.; Lu, E.; Wang, L.; Liu, R.; Lu, W.; Zhang, L.-C. Mechanical behavior and phase transformation of  $\beta$ -type Ti-35Nb-2Ta-3Zr alloy fabricated by 3D-Printing. *J. Alloys Compd.* **2019**, *790*, 117–126. [[CrossRef](#)]
26. Yang, Y.; Wang, G.; Liang, H.; Gao, C.; Peng, S.; Shen, L.; Shuai, C. Additive manufacturing of bone scaffolds. *Int. J. Bioprint* **2019**, *5*, 148. [[CrossRef](#)]
27. Revilla-León, M.; Meyer, M.J.; Özcan, M. Metal additive manufacturing technologies: Literature review of current status and prosthodontic applications. *Int. J. Comput. Dent.* **2019**, *22*, 55–67. [[PubMed](#)]
28. Maharubin, S.; Hu, Y.; Sooriyaarachchi, D.; Cong, W.; Tan, G.Z. Laser engineered net shaping of antimicrobial and biocompatible titanium-silver alloys. *Mater. Sci. Eng. C Mater. Biol. Appl.* **2019**, *105*, 110059. [[CrossRef](#)]
29. Mitun, D.; Balla, V.K.; Dwaipayyan, S.; Devika, D.; Manivasagam, G. Surface properties and cytocompatibility of Ti-6Al-4V fabricated using Laser Engineered Net Shaping. *Mater. Sci. Eng. C Mater. Biol. Appl.* **2019**, *100*, 104–116. [[CrossRef](#)]
30. Mangano, F.; Chambrone, L.; van Noort, R.; Miller, C.; Hatton, P.; Mangano, C. Direct metal laser sintering titanium dental implants: A review of the current literature. *Int. J. Biomater.* **2014**, *2014*, 461534. [[CrossRef](#)]
31. Venkatesh, K.V.; Nandini, V.V. Direct metal laser sintering: A digitised metal casting technology. *J. Indian Prosthodont. Soc.* **2013**, *13*, 389–392. [[CrossRef](#)] [[PubMed](#)]
32. Sarker, A.; Leary, M.; Fox, K. Metallic additive manufacturing for bone-interfacing implants. *Biointerphases* **2020**, *15*. [[CrossRef](#)]
33. Razavykia, A.; Brusa, E.; Delprete, C.; Yavari, R. An Overview of Additive Manufacturing Technologies—A Review to Technical Synthesis in Numerical Study of Selective Laser Melting. *Materials* **2020**, *13*, 3895. [[CrossRef](#)] [[PubMed](#)]
34. Atae, A.; Li, Y.; Song, G.; Wen, C. Metal Scaffolds Processed by Electron Beam Melting for Biomedical Applications. In *Metallic Foam Bone*; Woodhead Publishing: Cambridge, UK, 2017; pp. 83–110.
35. Dobbstein, H.; Gurevich, E.L.; George, E.P.; Ostendorf, A.; Laplanche, G. Laser metal deposition of compositionally graded TiZrNbTa refractory high-entropy alloys using elemental powder blends. *Addit. Manuf.* **2019**, *25*, 252–262. [[CrossRef](#)]
36. Arabnejad, S.; Johnston, B.; Tanzer, M.; Pasini, D. Fully porous 3D printed titanium femoral stem to reduce stress-shielding following total hip arthroplasty. *J. Orthop. Res.* **2017**, *35*, 1774–1783. [[CrossRef](#)]
37. Glassman, A.H.; Bobyn, J.D.; Tanzer, M. New femoral designs: Do they influence stress shielding? *Clin. Orthop. Relat. Res.* **2006**, *453*, 64–74. [[CrossRef](#)]
38. Liang, H.; Yang, Y.; Xie, D.; Li, L.; Mao, N.; Wang, C.; Tian, Z.; Jiang, Q.; Shen, L. Trabecular-like Ti-6Al-4V scaffolds for orthopedic: Fabrication by selective laser melting and in vitro biocompatibility. *J. Mater. Sci. Technol.* **2019**, *35*, 1284–1297. [[CrossRef](#)]
39. Wang, X.; Xu, S.; Zhou, S.; Xu, W.; Leary, M.; Choong, P.; Qian, M.; Brandt, M.; Xie, Y.M. Topological design and additive manufacturing of porous metals for bone scaffolds and orthopaedic implants: A review. *Biomaterials* **2016**, *83*, 127–141. [[CrossRef](#)]
40. Cheng, A.; Humayun, A.; Boyan, B.D.; Schwartz, Z. Enhanced Osteoblast Response to Porosity and Resolution of Additively Manufactured Ti-6Al-4V Constructs with Trabeculae-Inspired Porosity. *3d Print Addit Manuf.* **2016**, *3*, 10–21. [[CrossRef](#)]
41. Karageorgiou, V.; Kaplan, D. Porosity of 3D biomaterial scaffolds and osteogenesis. *Biomaterials* **2005**, *26*, 5474–5491. [[CrossRef](#)]
42. Kuboki, Y.; Takita, H.; Kobayashi, D.; Tsuruga, E.; Inoue, M.; Murata, M.; Nagai, N.; Dohi, Y.; Ohgushi, H. BMP-induced osteogenesis on the surface of hydroxyapatite with geometrically feasible and nonfeasible structures: Topology of osteogenesis. *J. Biomed. Mater. Res.* **1998**, *39*, 190–199. [[CrossRef](#)]
43. Gotz, H.E.; Muller, M.; Emmel, A.; Holzwarth, U.; Erben, R.G.; Stangl, R. Effect of surface finish on the osseointegration of laser-treated titanium alloy implants. *Biomaterials* **2004**, *25*, 4057–4064. [[CrossRef](#)]
44. Bobbert, F.S.L.; Zadpoor, A.A. Effects of bone substitute architecture and surface properties on cell response, angiogenesis, and structure of new bone. *J. Mater. Chem B* **2017**, *5*, 6175–6192. [[CrossRef](#)]
45. Zadpoor, A.A. Additively manufactured porous metallic biomaterials. *J. Mater. Chem B* **2019**, *7*, 4088–4117. [[CrossRef](#)]
46. van Hengel, I.A.J.; Riool, M.; Fratila-Apachitei, L.E.; Witte-Bouma, J.; Farrell, E.; Zadpoor, A.A.; Zaat, S.A.J.; Apachitei, I. Selective laser melting porous metallic implants with immobilized silver nanoparticles kill and prevent biofilm formation by methicillin-resistant *Staphylococcus aureus*. *Biomaterials* **2017**, *140*, 1–15. [[CrossRef](#)] [[PubMed](#)]
47. Ranganathan, S.I.; Kohama, C.; Mercurio, T.; Salvatore, A.; Benmassaoud, M.M.; Kim, T.W.B. Effect of temperature and ultraviolet light on the bacterial kill effectiveness of antibiotic-infused 3D printed implants. *Biomed. Microdevices* **2020**, *22*, 59. [[CrossRef](#)] [[PubMed](#)]
48. Chen, X.; Gao, C.; Jiang, J.; Wu, Y.; Zhu, P.; Chen, G. 3D printed porous PLA/nHA composite scaffolds with enhanced osteogenesis and osteoconductivity in vivo for bone regeneration. *Biomed. Mater.* **2019**, *14*, 065003. [[CrossRef](#)]
49. Wang, Y.; Wang, S.; Zhang, Y.; Mi, J.; Ding, X. Synthesis of Dimethyl Octyl Aminoethyl Ammonium Bromide and Preparation of Antibacterial ABS Composites for Fused Deposition Modeling. *Polymers* **2020**, *12*, 2229. [[CrossRef](#)]
50. Zeng, W.; He, J.; Liu, F. Preparation and properties of antibacterial ABS plastics based on polymeric quaternary phosphonium salts antibacterial agents. *Polym. Adv. Technol.* **2019**, *30*, 2515–2522. [[CrossRef](#)]

51. Mania, S.; Ryl, J.; Jinn, J.R.; Wang, Y.J.; Michałowska, A.; Tylingo, R. The Production Possibility of the Antimicrobial Filaments by Co-Extrusion of the PLA Pellet with Chitosan Powder for FDM 3D Printing Technology. *Polymers* **2019**, *11*, 1893. [[CrossRef](#)] [[PubMed](#)]
52. Yang, F.; Zeng, J.; Long, H.; Xiao, J.; Luo, Y.; Gu, J.; Zhou, W.; Wei, Y.; Dong, X. Micrometer Copper-Zinc Alloy Particles-Reinforced Wood Plastic Composites with High Gloss and Antibacterial Properties for 3D Printing. *Polymers* **2020**, *12*, 621. [[CrossRef](#)]
53. Sarker, A.; Nhiem, T.; Rifai, A.; Brandt, M.; Tran, P.A.; Leary, M.; Fox, K.; Williams, R. Rational design of additively manufactured Ti6Al4V implants to control Staphylococcus aureus biofilm formation. *Materialia* **2019**, *5*. [[CrossRef](#)]
54. Ganjian, M.; Modaresifar, K.; Ligeon, M.R.O.; Kunkels, L.B.; Tumer, N.; Angeloni, L.; Hagen, C.W.; Otten, L.C.; Hagedoorn, P.-L.; Apachitei, I.; et al. Nature Helps: Toward Bioinspired Bactericidal Nanopatterns. *Adv. Mater. Interfaces* **2019**, *6*. [[CrossRef](#)]
55. Chen, M.; Zhang, E.; Zhang, L. Microstructure, mechanical properties, bio-corrosion properties and antibacterial properties of Ti-Ag sintered alloys. *Mater. Sci Eng. C Mater. Biol. Appl.* **2016**, *62*, 350–360. [[CrossRef](#)] [[PubMed](#)]
56. Oliver, J.D.; Eells, A.C.; Saba, E.S.; Boczar, D.; Restrepo, D.J.; Huayllani, M.T.; Sisti, A.; Hu, M.S.; Gould, D.J.; Forte, A.J. Alloplastic Facial Implants: A Systematic Review and Meta-Analysis on Outcomes and Uses in Aesthetic and Reconstructive Plastic Surgery. *Aesthetic Plast. Surg.* **2019**, *43*, 625–636. [[CrossRef](#)]
57. Hemmilä, M.; Karvonen, M.; Laaksonen, I.; Matilainen, M.; Eskelinen, A.; Haapakoski, J.; Puhto, A.P.; Kettunen, J.; Manninen, M.; Mäkelä, K.T. Survival of 11,390 Continuum cups in primary total hip arthroplasty based on data from the Finnish Arthroplasty Register. *Acta Orthop.* **2019**, *90*, 312–317. [[CrossRef](#)]
58. Laaksonen, I.; Lorimer, M.; Gromov, K.; Eskelinen, A.; Rolfson, O.; Graves, S.E.; Malchau, H.; Mohaddes, M. Trabecular metal acetabular components in primary total hip arthroplasty. *Acta Orthop.* **2018**, *89*, 259–264. [[CrossRef](#)] [[PubMed](#)]
59. Matharu, G.S.; Judge, A.; Murray, D.W.; Pandit, H.G. Trabecular Metal Versus Non-Trabecular Metal Acetabular Components and the Risk of Re-Revision Following Revision Total Hip Arthroplasty: A Propensity Score-Matched Study from the National Joint Registry for England and Wales. *J. Bone Jt. Surg. Am.* **2018**, *100*, 1132–1140. [[CrossRef](#)]
60. Pingueiro, J.; Piattelli, A.; Paiva, J.; Figueiredo, L.C.; Feres, M.; Shibli, J.; Bueno-Silva, B. Additive manufacturing of titanium alloy could modify the pathogenic microbial profile: An in vitro study. *Braz Oral Res.* **2019**, *33*, e065. [[CrossRef](#)]
61. Koutiri, I.; Pessard, E.; Peyre, P.; Amlou, O.; De Terris, T. Influence of SLM process parameters on the surface finish, porosity rate and fatigue behavior of as-built Inconel 625 parts. *J. Mater. Process. Technol.* **2018**, *255*, 536–546. [[CrossRef](#)]
62. Villapun, V.M.; Carter, L.N.; Gao, N.; Addison, O.; Webber, M.A.; Shepherd, D.E.T.; Andrews, J.W.; Lowther, M.; Avery, S.; Glanvill, S.J.; et al. A design approach to facilitate selective attachment of bacteria and mammalian cells to additively manufactured implants. *Addit. Manuf.* **2020**, *36*, 12. [[CrossRef](#)]
63. Sarker, A.; Tran, N.; Rifai, A.; Elambasseril, J.; Brandt, M.; Williams, R.; Leary, M.; Fox, K. Angle defines attachment: Switching the biological response to titanium interfaces by modifying the inclination angle during selective laser melting. *Mater. Des.* **2018**, *154*, 326–339. [[CrossRef](#)]
64. Ginestra, P.; Ferraro, R.M.; Zohar-Hauber, K.; Abeni, A.; Giliani, S.; Ceretti, E. Selective Laser Melting and Electron Beam Melting of Ti6Al4V for Orthopedic Applications: A Comparative Study on the Applied Building Direction. *Materials* **2020**, *13*, 5584. [[CrossRef](#)]
65. Xie, K.; Guo, Y.; Zhao, S.; Wang, L.; Wu, J.; Tan, J.; Yang, Y.; Wu, W.; Jiang, W.; Hao, Y. Partially Melted Ti6Al4V Particles Increase Bacterial Adhesion and Inhibit Osteogenic Activity on 3D-printed Implants: An In Vitro Study. *Clin. Orthop. Relat. Res.* **2019**, *477*, 2772–2782. [[CrossRef](#)]
66. Ginestra, P.; Ceretti, E.; Lobo, D.; Lowther, M.; Cruchley, S.; Kuehne, S.; Villapun, V.; Cox, S.; Grover, L.; Shepherd, D.; et al. Post Processing of 3D Printed Metal Scaffolds: A Preliminary Study of Antimicrobial Efficiency. *Procedia Manuf.* **2020**, *47*, 1106–1112. [[CrossRef](#)]
67. Szymczyk, P.; Junka, A.; Ziolkowski, G.; Smutnicka, D.; Bartoszewicz, M.; Chlebus, E. The ability of *S. aureus* to form biofilm on the Ti-6Al-7Nb scaffolds produced by Selective Laser Melting and subjected to the different types of surface modifications. *Acta Bioeng. Biomech.* **2013**, *15*, 69–76. [[CrossRef](#)]
68. Junka, A.F.; Szymczyk, P.; Secewicz, A.; Pawlak, A.; Smutnicka, D.; Ziolkowski, G.; Bartoszewicz, M.; Chlebus, E. The chemical digestion of Ti6Al7Nb scaffolds produced by Selective Laser Melting reduces significantly ability of Pseudomonas aeruginosa to form biofilm. *Acta Bioeng. Biomech.* **2016**, *18*, 115–120. [[CrossRef](#)]
69. Cox, S.C.; Jamshidi, P.; Eisenstein, N.M.; Webber, M.A.; Burton, H.; Moakes, R.J.A.; Addison, O.; Attallah, M.; Shepherd, D.E.T.; Grover, L.M. Surface Finish has a Critical Influence on Biofilm Formation and Mammalian Cell Attachment to Additively Manufactured Prosthetics. *ACS Biomater. Sci. Eng.* **2017**, *3*, 1616–1626. [[CrossRef](#)] [[PubMed](#)]
70. Szymczyk-Ziolkowska, P.; Hoppe, V.; Rusinska, M.; Gasiorek, J.; Ziolkowski, G.; Dydak, K.; Czajkowska, J.; Junka, A. The Impact of EBM-Manufactured Ti6Al4V ELI Alloy Surface Modifications on Cytotoxicity toward Eukaryotic Cells and Microbial Biofilm Formation. *Materials* **2020**, *13*, 2822. [[CrossRef](#)] [[PubMed](#)]
71. Wang, Q.; Zhou, P.; Liu, S.; Attarilar, S.; Ma, R.L.; Zhong, Y.; Wang, L. Multi-Scale Surface Treatments of Titanium Implants for Rapid Osseointegration: A Review. *Nanomaterials* **2020**, *10*, 1244. [[CrossRef](#)]
72. Skoric, L.; Sanz-Hernandez, D.; Meng, F.; Donnelly, C.; Merino-Aceituno, S.; Fernandez-Pacheco, A. Layer-by-Layer Growth of Complex-Shaped Three-Dimensional Nanostructures with Focused Electron Beams. *Nano Lett.* **2020**, *20*, 184–191. [[CrossRef](#)]
73. Liao, C.; Wuethrich, A.; Trau, M. A material odyssey for 3D nano/microstructures: Two photon polymerization based nanolithography in bioapplications. *Appl. Mater. Today* **2020**, *19*. [[CrossRef](#)]

74. Raimondi, M.T.; Eaton, S.M.; Nava, M.M.; Lagana, M.; Cerullo, G.; Osellame, R. Two-photon laser polymerization: From fundamentals to biomedical application in tissue engineering and regenerative medicine. *J. Appl. Biomater. Funct. Mater.* **2012**, *10*, 55–65. [[CrossRef](#)] [[PubMed](#)]
75. van Dorp, W.F.; van Someren, B.; Hagen, C.W.; Kruit, P.; Crozier, P.A. Approaching the resolution limit of nanometer-scale electron beam-induced deposition. *Nano Lett.* **2005**, *5*, 1303–1307. [[CrossRef](#)] [[PubMed](#)]
76. Utke, I.; Hoffmann, P.; Melngailis, J. Gas-assisted focused electron beam and ion beam processing and fabrication. *J. Vac. Sci. Technol. B Microelectron. Nanometer Struct.* **2008**, *26*. [[CrossRef](#)]
77. Plank, H.; Winkler, R.; Schwalb, C.H.; Hutner, J.; Fowlkes, J.D.; Rack, P.D.; Utke, I.; Huth, M. Focused Electron Beam-Based 3D Nanoprinting for Scanning Probe Microscopy: A Review. *Micromachines* **2019**, *11*, 48. [[CrossRef](#)] [[PubMed](#)]
78. Xing, J.F.; Zheng, M.L.; Duan, X.M. Two-photon polymerization microfabrication of hydrogels: An advanced 3D printing technology for tissue engineering and drug delivery. *Chem Soc. Rev.* **2015**, *44*, 5031–5039. [[CrossRef](#)]
79. Kumeria, T.; Gulati, K.; Santos, A.; Losic, D. Real-time and in situ drug release monitoring from nanoporous implants under dynamic flow conditions by reflectometric interference spectroscopy. *ACS Appl Mater. Interfaces* **2013**, *5*, 5436–5442. [[CrossRef](#)]
80. Gulati, K.; Aw, M.S.; Findlay, D.; Losic, D. Local drug delivery to the bone by drug-releasing implants: Perspectives of nano-engineered titania nanotube arrays. *Ther. Deliv.* **2012**, *3*, 857–873. [[CrossRef](#)]
81. King, D.; McGinty, S. Assessing the potential of mathematical modelling in designing drug-releasing orthopaedic implants. *J. Control Release* **2016**, *239*, 49–61. [[CrossRef](#)]
82. Park, Y.S.; Cho, J.Y.; Lee, S.J.; Hwang, C.I. Modified titanium implant as a gateway to the human body: The implant mediated drug delivery system. *Biomed. Res. Int.* **2014**, *2014*, 801358. [[CrossRef](#)] [[PubMed](#)]
83. Gimeno, M.; Pinczowski, P.; Vazquez, F.J.; Perez, M.; Santamaria, J.; Arruebo, M.; Lujan, L. Porous orthopedic steel implant as an antibiotic eluting device: Prevention of post-surgical infection on an ovine model. *Int. J. Pharm.* **2013**, *452*, 166–172. [[CrossRef](#)] [[PubMed](#)]
84. Gimeno, M.; Pinczowski, P.; Perez, M.; Giorello, A.; Martinez, M.A.; Santamaria, J.; Arruebo, M.; Lujan, L. A controlled antibiotic release system to prevent orthopedic-implant associated infections: An in vitro study. *Eur. J. Pharm. Biopharm.* **2015**, *96*, 264–271. [[CrossRef](#)] [[PubMed](#)]
85. Cox, S.C.; Jamshidi, P.; Eisenstein, N.M.; Webber, M.A.; Hassanin, H.; Attallah, M.M.; Shepherd, D.E.T.; Addison, O.; Grover, L.M. Adding functionality with additive manufacturing: Fabrication of titanium-based antibiotic eluting implants. *Mater. Sci Eng. C Mater. Biol. Appl.* **2016**, *64*, 407–415. [[CrossRef](#)] [[PubMed](#)]
86. Hassanin, H.; Finet, L.; Cox, S.C.; Jamshidi, P.; Grover, L.M.; Shepherd, D.E.T.; Addison, O.; Attallah, M.M. Tailoring selective laser melting process for titanium drug-delivering implants with releasing micro-channels. *Addit. Manuf.* **2018**, *20*, 144–155. [[CrossRef](#)]
87. Bezuidenhout, M.B.; van Staden, A.D.; Oosthuizen, G.A.; Dimitrov, D.M.; Dicks, L.M. Delivery of antibiotics from cementless titanium-alloy cubes may be a novel way to control postoperative infections. *Biomed. Res. Int.* **2015**, *2015*, 856859. [[CrossRef](#)]
88. Bezuidenhout, M.B.; Booyesen, E.; van Staden, A.D.; Uheida, E.H.; Hugo, P.A.; Oosthuizen, G.A.; Dimitrov, D.M.; Dicks, L.M.T. Selective Laser Melting of Integrated Ti6Al4V ELI Permeable Walls for Controlled Drug Delivery of Vancomycin. *ACS Biomater. Sci. Eng.* **2018**, *4*, 4412–4424. [[CrossRef](#)]
89. Perez, L.M.; Lalueva, P.; Monzon, M.; Puertolas, J.A.; Arruebo, M.; Santamaria, J. Hollow porous implants filled with mesoporous silica particles as a two-stage antibiotic-eluting device. *Int. J. Pharm.* **2011**, *409*, 1–8. [[CrossRef](#)]
90. Benmassaoud, M.M.; Kohama, C.; Kim, T.W.B.; Kadowec, J.A.; Foltiny, B.; Mercurio, T.; Ranganathan, S.I. Efficacy of eluted antibiotics through 3D printed femoral implants. *Biomed. Microdevices* **2019**, *21*, 51. [[CrossRef](#)]
91. Burton, H.E.; Eisenstein, N.M.; Lawless, B.M.; Jamshidi, P.; Segarra, M.A.; Addison, O.; Shepherd, D.E.T.; Attallah, M.M.; Grover, L.M.; Cox, S.C. The design of additively manufactured lattices to increase the functionality of medical implants. *Mater. Sci. Eng. C Mater. Biol. Appl.* **2019**, *94*, 901–908. [[CrossRef](#)]
92. Sukhorukova, I.V.; Sheveyko, A.N.; Kiryukhantsev-Korneev, P.V.; Anisimova, N.Y.; Gloushankova, N.A.; Zhitnyak, I.Y.; Benesova, J.; Amler, E.; Shtansky, D.V. Two approaches to form antibacterial surface: Doping with bactericidal element and drug loading. *Appl. Surf. Sci.* **2015**, *330*, 339–350. [[CrossRef](#)]
93. Souza, J.G.S.; Bertolini, M.M.; Costa, R.C.; Nagay, B.E.; Dongari-Bagtzoglou, A.; Barão, V.A.R. Targeting implant-associated infections: Titanium surface loaded with antimicrobial. *iScience* **2021**, *24*, 102008. [[CrossRef](#)] [[PubMed](#)]
94. Chen, L.; Song, X.; Xing, F.; Wang, Y.; Wang, Y.; He, Z.; Sun, L. A Review on Antimicrobial Coatings for Biomaterial Implants and Medical Devices. *J. Biomed. Nanotechnol.* **2020**, *16*, 789–809. [[CrossRef](#)] [[PubMed](#)]
95. Rodriguez-Contreras, A.; Torres, D.; Guillem-Marti, J.; Sereno, P.; Pau-Ginebra, M.; Calero, J.A.; Maria Manero, J.; Ruperez, E. Development of novel dual-action coatings with osteoinductive and antibacterial properties for 3D-printed titanium implants. *Surf. Coat. Technol.* **2020**, *403*. [[CrossRef](#)]
96. Yadav, S.K.; Khan, G.; Mishra, B. Advances in patents related to intrapocket technology for the management of periodontitis. *Recent Pat. Drug Deliv.* **2015**, *9*, 129–145. [[CrossRef](#)] [[PubMed](#)]
97. Ma, M.; Kazemzadeh-Narbat, M.; Hui, Y.; Lu, S.; Ding, C.; Chen, D.D.; Hancock, R.E.; Wang, R. Local delivery of antimicrobial peptides using self-organized TiO<sub>2</sub> nanotube arrays for peri-implant infections. *J. Biomed. Mater. Res. A* **2012**, *100*, 278–285. [[CrossRef](#)] [[PubMed](#)]

98. Goodman, S.B.; Yao, Z.; Keeney, M.; Yang, F. The future of biologic coatings for orthopaedic implants. *Biomaterials* **2013**, *34*, 3174–3183. [[CrossRef](#)]
99. de Jonge, L.T.; Leeuwenburgh, S.C.; Wolke, J.G.; Jansen, J.A. Organic-inorganic surface modifications for titanium implant surfaces. *Pharm Res.* **2008**, *25*, 2357–2369. [[CrossRef](#)]
100. Barik, A.; Chakravorty, N. Targeted Drug Delivery from Titanium Implants: A Review of Challenges and Approaches. *Adv. Exp. Med. Biol.* **2020**, *1251*, 1–17. [[CrossRef](#)]
101. Zhang, L.-C.; Chen, L.-Y.; Wang, L. Surface Modification of Titanium and Titanium Alloys: Technologies, Developments, and Future Interests. *Adv. Eng. Mater.* **2020**, *22*. [[CrossRef](#)]
102. Han, C.; Yao, Y.; Cheng, X.; Luo, J.; Luo, P.; Wang, Q.; Yang, F.; Wei, Q.; Zhang, Z. Electrophoretic Deposition of Gentamicin-Loaded Silk Fibroin Coatings on 3D-Printed Porous Cobalt-Chromium-Molybdenum Bone Substitutes to Prevent Orthopedic Implant Infections. *Biomacromolecules* **2017**, *18*, 3776–3787. [[CrossRef](#)]
103. Liu, J.; Liu, J.; Attarilar, S.; Wang, C.; Tamaddon, M.; Yang, C.; Xie, K.; Yao, J.; Wang, L.; Liu, C.; et al. Nano-Modified Titanium Implant Materials: A Way Toward Improved Antibacterial Properties. *Front. Bioeng. Biotechnol.* **2020**, *8*, 576969. [[CrossRef](#)]
104. Popat, K.C.; Eltgroth, M.; LaTempa, T.J.; Grimes, C.A.; Desai, T.A. Titania nanotubes: A novel platform for drug-eluting coatings for medical implants? *Small* **2007**, *3*, 1878–1881. [[CrossRef](#)] [[PubMed](#)]
105. Hu, X.; Xu, R.; Yu, X.; Chen, J.; Wan, S.; Ouyang, J.; Deng, F. Enhanced antibacterial efficacy of selective laser melting titanium surface with nanophase calcium phosphate embedded to TiO<sub>2</sub> nanotubes. *Biomed. Mater.* **2018**, *13*, 045015. [[CrossRef](#)] [[PubMed](#)]
106. Gao, A.; Hang, R.; Huang, X.; Zhao, L.; Zhang, X.; Wang, L.; Tang, B.; Ma, S.; Chu, P.K. The effects of titania nanotubes with embedded silver oxide nanoparticles on bacteria and osteoblasts. *Biomaterials* **2014**, *35*, 4223–4235. [[CrossRef](#)] [[PubMed](#)]
107. Zhang, T.; Zhou, W.; Jia, Z.; Wei, Q.; Fan, D.; Yan, J.; Yin, C.; Cheng, Y.; Cai, H.; Liu, X.; et al. Polydopamine-assisted functionalization of heparin and vancomycin onto microarc-oxidized 3D printed porous Ti<sub>6</sub>Al<sub>4</sub>V for improved hemocompatibility, osteogenic and anti-infection potencies. *Sci. China-Mater.* **2018**, *61*, 579–592. [[CrossRef](#)]
108. Jia, Z.; Xiu, P.; Xiong, P.; Zhou, W.; Cheng, Y.; Wei, S.; Zheng, Y.; Xi, T.; Cai, H.; Liu, Z.; et al. Additively Manufactured Macroporous Titanium with Silver-Releasing Micro-/Nanoporous Surface for Multipurpose Infection Control and Bone Repair—A Proof of Concept. *ACS Appl. Mater. Interfaces* **2016**, *8*, 28495–28510. [[CrossRef](#)]
109. Jia, Z.; Li, M.; Xiu, P.; Xu, X.; Cheng, Y.; Zheng, Y.; Xi, T.; Wei, S.; Liu, Z. A novel cytocompatible, hierarchical porous Ti<sub>6</sub>Al<sub>4</sub>V scaffold with immobilized silver nanoparticles. *Mater. Lett.* **2015**, *157*, 143–146. [[CrossRef](#)]
110. Maher, S.; Kaur, G.; Lima-Marques, L.; Evdokiou, A.; Losic, D. Engineering of Micro- to Nanostructured 3D-Printed Drug-Releasing Titanium Implants for Enhanced Osseointegration and Localized Delivery of Anticancer Drugs. *ACS Appl. Mater. Interfaces* **2017**, *9*, 29562–29570. [[CrossRef](#)] [[PubMed](#)]
111. Gulati, K.; Prideaux, M.; Kogawa, M.; Lima-Marques, L.; Atkins, G.J.; Findlay, D.M.; Losic, D. Anodized 3D-printed titanium implants with dual micro- and nano-scale topography promote interaction with human osteoblasts and osteocyte-like cells. *J. Tissue Eng. Regen. Med.* **2017**, *11*, 3313–3325. [[CrossRef](#)]
112. Xue, T.; Attarilar, S.; Liu, S.; Liu, J.; Song, X.; Li, L.; Zhao, B.; Tang, Y. Surface Modification Techniques of Titanium and its Alloys to Functionally Optimize Their Biomedical Properties: Thematic Review. *Front. Bioeng. Biotechnol.* **2020**, *8*, 603072. [[CrossRef](#)]
113. Nair, M.; Elizabeth, E. Applications of Titania Nanotubes in Bone Biology. *J. Nanosci. Nanotechnol.* **2015**, *15*, 939–955. [[CrossRef](#)]
114. Ahn, T.K.; Lee, D.H.; Kim, T.S.; Jang, G.C.; Choi, S.; Oh, J.B.; Ye, G.; Lee, S. Modification of Titanium Implant and Titanium Dioxide for Bone Tissue Engineering. *Adv. Exp. Med. Biol.* **2018**, *1077*, 355–368. [[CrossRef](#)]
115. Popat, K.C.; Eltgroth, M.; Latempa, T.J.; Grimes, C.A.; Desai, T.A. Decreased Staphylococcus epidermidis adhesion and increased osteoblast functionality on antibiotic-loaded titania nanotubes. *Biomaterials* **2007**, *28*, 4880–4888. [[CrossRef](#)]
116. He, P.; Zhang, H.; Li, Y.; Ren, M.; Xiang, J.; Zhang, Z.; Ji, P.; Yang, S. 1 $\alpha$ ,25-Dihydroxyvitamin D<sub>3</sub>-loaded hierarchical titanium scaffold enhanced early osseointegration. *Mater. Sci. Eng. C Mater. Biol. Appl.* **2020**, *109*, 110551. [[CrossRef](#)] [[PubMed](#)]
117. Losic, D.; Simovic, S. Self-ordered nanopore and nanotube platforms for drug delivery applications. *Expert Opin. Drug. Deliv.* **2009**, *6*, 1363–1381. [[CrossRef](#)] [[PubMed](#)]
118. Maher, S.; Mazinani, A.; Barati, M.R.; Losic, D. Engineered titanium implants for localized drug delivery: Recent advances and perspectives of Titania nanotubes arrays. *Expert Opin. Drug. Deliv.* **2018**, *15*, 1021–1037. [[CrossRef](#)] [[PubMed](#)]
119. Kang, H.-J.; Kim, D.J.; Park, S.-J.; Yoo, J.-B.; Ryu, Y.S. Controlled drug release using nanoporous anodic aluminum oxide on stent. *Thin Solid Film.* **2007**, *515*, 5184–5187. [[CrossRef](#)]
120. Kumeria, T.; Mon, H.; Aw, M.S.; Gulati, K.; Santos, A.; Griesser, H.J.; Losic, D. Advanced biopolymer-coated drug-releasing titania nanotubes (TNTs) implants with simultaneously enhanced osteoblast adhesion and antibacterial properties. *Colloids Surf. B Biointerfaces* **2015**, *130*, 255–263. [[CrossRef](#)] [[PubMed](#)]
121. Li, Y.; Yang, Y.; Li, R.; Tang, X.; Guo, D.; Qing, Y.; Qin, Y. Enhanced antibacterial properties of orthopedic implants by titanium nanotube surface modification: A review of current techniques. *Int. J. Nanomed.* **2019**, *14*, 7217–7236. [[CrossRef](#)]
122. Maher, S.; Wijenayaka, A.R.; Lima-Marques, L.; Yang, D.; Atkins, G.J.; Losic, D. Advancing of Additive-Manufactured Titanium Implants with Bioinspired Micro- to Nanotopographies. *ACS Biomater. Sci. Eng.* **2021**, *7*, 441–450. [[CrossRef](#)]
123. Im, S.Y.; Kim, K.M.; Kwon, J.S. Antibacterial and Osteogenic Activity of Titania Nanotubes Modified with Electrospray-Deposited Tetracycline Nanoparticles. *Nanomaterials* **2020**, *10*, 1093. [[CrossRef](#)]
124. Han, L.; Wang, M.; Sun, H.; Li, P.; Wang, K.; Ren, F.; Lu, X. Porous titanium scaffolds with self-assembled micro/nano-hierarchical structure for dual functions of bone regeneration and anti-infection. *J. Biomed. Mater. Res. A* **2017**, *105*, 3482–3492. [[CrossRef](#)]

125. Guo, Z.; Chen, Y.; Wang, Y.; Jiang, H.; Wang, X. Advances and challenges in metallic nanomaterial synthesis and antibacterial applications. *J. Mater. Chem B* **2020**, *8*, 4764–4777. [[CrossRef](#)]
126. Surmeneva, M.; Lapanje, A.; Chudinova, E.; Ivanova, A.; Koptuyug, A.; Loza, K.; Prymak, O.; Epple, M.; Ennen-Roth, F.; Ulbricht, M.; et al. Decreased bacterial colonization of additively manufactured Ti6Al4V metallic scaffolds with immobilized silver and calcium phosphate nanoparticles. *Appl. Surf. Sci.* **2019**, *480*, 822–829. [[CrossRef](#)]
127. Rifai, A.; Tran, N.; Reineck, P.; Elbourne, A.; Mayes, E.; Sarker, A.; Dekiwadia, C.; Ivanova, E.P.; Crawford, R.J.; Ohshima, T.; et al. Engineering the Interface: Nanodiamond Coating on 3D-Printed Titanium Promotes Mammalian Cell Growth and Inhibits Staphylococcus aureus Colonization. *ACS Appl Mater. Interfaces* **2019**, *11*, 24588–24597. [[CrossRef](#)]
128. Bakhshandeh, S.; Gorgin Karaji, Z.; Lietaert, K.; Fluit, A.C.; Boel, C.H.E.; Vogely, H.C.; Vermonden, T.; Hennink, W.E.; Weinans, H.; Zadpoor, A.A.; et al. Simultaneous Delivery of Multiple Antibacterial Agents from Additively Manufactured Porous Biomaterials to Fully Eradicate Planktonic and Adherent Staphylococcus aureus. *ACS Appl. Mater. Interfaces* **2017**, *9*, 25691–25699. [[CrossRef](#)]
129. Griseti, Q.; Jacquet, C.; Sautet, P.; Abdel, M.P.; Parratte, S.; Ollivier, M.; Argenson, J.N. Antimicrobial properties of antibiotic-loaded implants a comparative study of antimicrobial properties of antibiotic-loaded cement, tantalum, 3D-printed porous titanium, and titanium alloy. *Bone Jt. J.* **2020**, *102B*, 158–162. [[CrossRef](#)]
130. Anguita-Alonso, P.; Hanssen, A.D.; Osmon, D.R.; Trampuz, A.; Steckelberg, J.M.; Patel, R. High rate of aminoglycoside resistance among staphylococci causing prosthetic joint infection. *Clin. Orthop. Relat. Res.* **2005**, *439*, 43–47. [[CrossRef](#)]
131. Chen, A.F.; Parvizi, J. Antibiotic-loaded bone cement and periprosthetic joint infection. *J. Long Term Eff. Med. Implant.* **2014**, *24*, 89–97. [[CrossRef](#)]
132. Srinivasan, A.; Dick, J.D.; Perl, T.M. Vancomycin resistance in staphylococci. *Clin. Microbiol. Rev.* **2002**, *15*, 430–438. [[CrossRef](#)] [[PubMed](#)]
133. Molina-Manso, D.; del Prado, G.; Ortiz-Pérez, A.; Manrubia-Cobo, M.; Gómez-Barrena, E.; Cordero-Ampuero, J.; Esteban, J. In vitro susceptibility to antibiotics of staphylococci in biofilms isolated from orthopaedic infections. *Int. J. Antimicrob. Agents* **2013**, *41*, 521–523. [[CrossRef](#)] [[PubMed](#)]
134. Sawada, M.; Oe, K.; Hirata, M.; Kawamura, H.; Ueda, N.; Nakamura, T.; Iida, H.; Saito, T. Linezolid versus daptomycin treatment for periprosthetic joint infections: A retrospective cohort study. *J. Orthop. Surg. Res.* **2019**, *14*, 334. [[CrossRef](#)]
135. Chen, C.P.; Jing, R.Y.; Wickstrom, E. Covalent Attachment of Daptomycin to Ti6Al4V Alloy Surfaces by a Thioether Linkage to Inhibit Colonization by *Staphylococcus aureus*. *ACS Omega* **2017**, *2*, 1645–1652. [[CrossRef](#)]
136. Lv, H.; Chen, Z.; Yang, X.; Cen, L.; Zhang, X.; Gao, P. Layer-by-layer self-assembly of minocycline-loaded chitosan/alginate multilayer on titanium substrates to inhibit biofilm formation. *J. Dent.* **2014**, *42*, 1464–1472. [[CrossRef](#)]
137. Raad, I.; Hanna, H.; Jiang, Y.; Dvorak, T.; Reitzel, R.; Chaiban, G.; Sherertz, R.; Hachem, R. Comparative activities of daptomycin, linezolid, and tigecycline against catheter-related methicillin-resistant *Staphylococcus bacteremic* isolates embedded in biofilm. *Antimicrob. Agents Chemother.* **2007**, *51*, 1656–1660. [[CrossRef](#)]
138. Stigter, M.; Bezemer, J.; de Groot, K.; Layrolle, P. Incorporation of different antibiotics into carbonated hydroxyapatite coatings on titanium implants, release and antibiotic efficacy. *J. Control Release* **2004**, *99*, 127–137. [[CrossRef](#)]
139. Croes, M.; Bakhshandeh, S.; van Hengel, I.A.J.; Lietaert, K.; van Kessel, K.P.M.; Pouran, B.; van der Wal, B.C.H.; Vogely, H.C.; Van Hecke, W.; Fluit, A.C.; et al. Antibacterial and immunogenic behavior of silver coatings on additively manufactured porous titanium. *Acta Biomater.* **2018**, *81*, 315–327. [[CrossRef](#)]
140. Yavari, S.A.; Croes, M.; Akhavan, B.; Jahanmard, F.; Eigenhuis, C.C.; Dadbakhsh, S.; Vogely, H.C.; Bilek, M.M.; Fluit, A.C.; Boel, C.H.E.; et al. Layer by layer coating for bio-functionalization of additively manufactured meta-biomaterials. *Addit. Manuf.* **2020**, *32*. [[CrossRef](#)]
141. Guan, B.; Wang, H.; Xu, R.; Zheng, G.; Yang, J.; Liu, Z.; Cao, M.; Wu, M.; Song, J.; Li, N.; et al. Establishing Antibacterial Multilayer Films on the Surface of Direct Metal Laser Sintered Titanium Primed with Phase-Transited Lysozyme. *Sci. Rep.* **2016**, *6*, 36408. [[CrossRef](#)]
142. Jahanmard, F.; Croes, M.; Castilho, M.; Majed, A.; Steenbergen, M.J.; Lietaert, K.; Vogely, H.C.; van der Wal, B.C.H.; Stapels, D.A.C.; Malda, J.; et al. Bactericidal coating to prevent early and delayed implant-related infections. *J. Control Release* **2020**, *326*, 38–52. [[CrossRef](#)]
143. Jahanmard, F.; Dijkmans, F.M.; Majed, A.; Vogely, H.C.; van der Wal, B.C.H.; Stapels, D.A.C.; Ahmadi, S.M.; Vermonden, T.; Amin Yavari, S. Toward Antibacterial Coatings for Personalized Implants. *ACS Biomater. Sci. Eng.* **2020**, *6*, 5486–5492. [[CrossRef](#)]
144. Dong, J.; Zhang, S.; Liu, H.; Li, X.; Liu, Y.; Du, Y. Novel alternative therapy for spinal tuberculosis during surgery: Reconstructing with anti-tuberculosis bioactivity implants. *Expert Opin. Drug Deliv.* **2014**, *11*, 299–305. [[CrossRef](#)]
145. Ghimire, N.; Luo, J.; Tang, R.; Sun, Y.; Deng, Y. Novel anti-infective activities of chitosan immobilized titanium surface with enhanced osteogenic properties. *Colloids Surf. B Biointerfaces* **2014**, *122*, 126–133. [[CrossRef](#)]
146. Karaji, Z.G.; Jahanmard, F.; Mirzaei, A.H.; van der Wal, B.; Yavari, S.A. A multifunctional silk coating on additively manufactured porous titanium to prevent implant-associated infection and stimulate bone regeneration. *Biomed. Mater.* **2020**, *15*. [[CrossRef](#)]
147. Dydak, K.; Junka, A.; Szymczyk, P.; Chodaczek, G.; Toporkiewicz, M.; Fijałkowski, K.; Dudek, B.; Bartoszewicz, M. Development and biological evaluation of Ti6Al7Nb scaffold implants coated with gentamycin-saturated bacterial cellulose biomaterial. *PLoS ONE* **2018**, *13*, e0205205. [[CrossRef](#)]
148. Zhang, Y.; Xu, Z.; Suo, H.; Feng, W. [Research progress of drug-loaded antibacterial coating of orthopedic metal implants]. *Zhongguo Xiu Fu Chong Jian Wai Ke Za Zhi* **2017**, *31*, 1396–1401. [[CrossRef](#)] [[PubMed](#)]

149. Choi, H.; Schulte, A.; Muller, M.; Park, M.; Jo, S.; Schonherr, H. Drug Release from Thermo-Responsive Polymer Brush Coatings to Control Bacterial Colonization and Biofilm Growth on Titanium Implants. *Adv. Healthc Mater.* **2021**, e2100069. [[CrossRef](#)] [[PubMed](#)]
150. Liu, Z.; Zhu, Y.; Liu, X.; Yeung, K.W.K.; Wu, S. Construction of poly (vinyl alcohol)/poly (lactide-glycolide acid)/vancomycin nanoparticles on titanium for enhancing the surface self-antibacterial activity and cytocompatibility. *Colloids Surf. B Biointerfaces* **2017**, *151*, 165–177. [[CrossRef](#)]
151. Shi, X.; Wu, H.; Li, Y.; Wei, X.; Du, Y. Electrical signals guided entrapment and controlled release of antibiotics on titanium surface. *J. Biomed. Mater. Res. A* **2013**, *101*, 1373–1378. [[CrossRef](#)]
152. Vaithilingam, J.; Kilsby, S.; Goodridge, R.D.; Christie, S.D.R.; Edmondson, S.; Hague, R.J.M. Immobilisation of an antibacterial drug to Ti6Al4V components fabricated using selective laser melting. *Appl. Surf. Sci.* **2014**, *314*, 642–654. [[CrossRef](#)]
153. Fiore, M.; Sambri, A.; Zucchini, R.; Giannini, C.; Donati, D.M.; De Paolis, M. Silver-coated megaprosthesis in prevention and treatment of peri-prosthetic infections: A systematic review and meta-analysis about efficacy and toxicity in primary and revision surgery. *Eur. J. Orthop. Surg. Traumatol.* **2021**, *31*, 201–220. [[CrossRef](#)]
154. Xiu, Z.M.; Zhang, Q.B.; Puppala, H.L.; Colvin, V.L.; Alvarez, P.J. Negligible particle-specific antibacterial activity of silver nanoparticles. *Nano Lett.* **2012**, *12*, 4271–4275. [[CrossRef](#)]
155. Rizzello, L.; Pompa, P.P. Nanosilver-based antibacterial drugs and devices: Mechanisms, methodological drawbacks, and guidelines. *Chem Soc. Rev.* **2014**, *43*, 1501–1518. [[CrossRef](#)]
156. Morones, J.R.; Elechiguerra, J.L.; Camacho, A.; Holt, K.; Kouri, J.B.; Ramírez, J.T.; Yacaman, M.J. The bactericidal effect of silver nanoparticles. *Nanotechnology* **2005**, *16*, 2346–2353. [[CrossRef](#)]
157. Choi, O.; Hu, Z. Size dependent and reactive oxygen species related nanosilver toxicity to nitrifying bacteria. *Env. Sci. Technol.* **2008**, *42*, 4583–4588. [[CrossRef](#)] [[PubMed](#)]
158. Sukhorukova, I.V.; Sheveyko, A.N.; Manakhov, A.; Zhitnyak, I.Y.; Gloushankova, N.A.; Denisenko, E.A.; Filippovich, S.Y.; Ignatov, S.G.; Shtansky, D.V. Synergistic and long-lasting antibacterial effect of antibiotic-loaded TiCaPCON-Ag films against pathogenic bacteria and fungi. *Mater. Sci. Eng. C Mater. Biol. Appl.* **2018**, *90*, 289–299. [[CrossRef](#)] [[PubMed](#)]
159. Shivaram, A.; Bose, S.; Bandyopadhyay, A. Understanding long-term silver release from surface modified porous titanium implants. *Acta Biomater.* **2017**, *58*, 550–560. [[CrossRef](#)]
160. Qiao, S.; Wu, D.; Li, Z.; Zhu, Y.; Zhan, F.; Lai, H.; Gu, Y. The combination of multi-functional ingredients-loaded hydrogels and three-dimensional printed porous titanium alloys for infective bone defect treatment. *J. Tissue Eng.* **2020**, *11*, 2041731420965797. [[CrossRef](#)]
161. Jia, Z.; Zhou, W.; Yan, J.; Xiong, P.; Guo, H.; Cheng, Y.; Zheng, Y. Constructing Multilayer Silk Protein/Nanosilver Biofunctionalized Hierarchically Structured 3D Printed Ti<sub>6</sub>Al<sub>4</sub>V Scaffold for Repair of Infective Bone Defects. *ACS Biomater. Sci. Eng.* **2019**, *5*, 244–261. [[CrossRef](#)]
162. Devlin-Mullin, A.; Todd, N.M.; Golrokhi, Z.; Geng, H.; Konerding, M.A.; Ternan, N.G.; Hunt, J.A.; Potter, R.J.; Sutcliffe, C.; Jones, E.; et al. Atomic Layer Deposition of a Silver Nanolayer on Advanced Titanium Orthopedic Implants Inhibits Bacterial Colonization and Supports Vascularized de Novo Bone Ingrowth. *Adv. Healthc. Mater.* **2017**, *6*. [[CrossRef](#)]
163. Amin Yavari, S.; Loozen, L.; Paganelli, F.L.; Bakhshandeh, S.; Lietaert, K.; Groot, J.A.; Fluit, A.C.; Boel, C.H.; Alblas, J.; Vogely, H.C.; et al. Antibacterial Behavior of Additively Manufactured Porous Titanium with Nanotubular Surfaces Releasing Silver Ions. *ACS Appl. Mater. Interfaces* **2016**, *8*, 17080–17089. [[CrossRef](#)] [[PubMed](#)]
164. Jia, Z.; Xiu, P.; Li, M.; Xu, X.; Shi, Y.; Cheng, Y.; Wei, S.; Zheng, Y.; Xi, T.; Cai, H.; et al. Bioinspired anchoring AgNPs onto micro-nanoporous TiO<sub>2</sub> orthopedic coatings: Trap-killing of bacteria, surface-regulated osteoblast functions and host responses. *Biomaterials* **2016**, *75*, 203–222. [[CrossRef](#)] [[PubMed](#)]
165. Morones-Ramirez, J.R.; Winkler, J.A.; Spina, C.S.; Collins, J.J. Silver enhances antibiotic activity against gram-negative bacteria. *Sci. Transl. Med.* **2013**, *5*, 190ra181. [[CrossRef](#)] [[PubMed](#)]
166. Bing, W.; Chen, Z.; Sun, H.; Shi, P.; Gao, N.; Ren, J.; Qu, X. Visible-light-driven enhanced antibacterial and biofilm elimination activity of graphitic carbon nitride by embedded Ag nanoparticles. *Nano Res.* **2015**, *8*, 1648–1658. [[CrossRef](#)]
167. Razzi, F.; Fratila-Apachitei, L.E.; Fahy, N.; Bastiaansen-Jenniskens, Y.M.; Apachitei, I.; Farrell, E.; Zadpoor, A.A. Immunomodulation of surface biofunctionalized 3D printed porous titanium implants. *Biomed. Mater.* **2020**, *15*, 035017. [[CrossRef](#)] [[PubMed](#)]
168. van Hengel, I.A.J.; Gelderman, F.S.A.; Athanasiadis, S.; Minneboo, M.; Weinans, H.; Fluit, A.C.; vander Eerden, B.C.J.; Fratila-Apachitei, L.E.; Apachitei, I.; Zadpoor, A.A. Functionality-packed additively manufactured porous titanium implants. *Mater. Today Bio.* **2020**, *7*. [[CrossRef](#)] [[PubMed](#)]
169. van Hengel, I.A.J.; Putra, N.E.; Tierolf, M.; Minneboo, M.; Fluit, A.C.; Fratila-Apachitei, L.E.; Apachitei, I.; Zadpoor, A.A. Biofunctionalization of selective laser melted porous titanium using silver and zinc nanoparticles to prevent infections by antibiotic-resistant bacteria. *Acta Biomater.* **2020**, *107*, 325–337. [[CrossRef](#)]
170. Shimabukuro, M. Antibacterial Property and Biocompatibility of Silver, Copper, and Zinc in Titanium Dioxide Layers Incorporated by One-Step Micro-Arc Oxidation: A Review. *Antibiotics* **2020**, *9*, 716. [[CrossRef](#)] [[PubMed](#)]
171. Krakhmalev, P.; Yadroitsev, I.; Yadroitsava, I.; de Smidt, O. Functionalization of Biomedical Ti6Al4V via In Situ Alloying by Cu during Laser Powder Bed Fusion Manufacturing. *Materials* **2017**, *10*, 1154. [[CrossRef](#)]
172. Liu, R.; Memarzadeh, K.; Chang, B.; Zhang, Y.; Ma, Z.; Allaker, R.P.; Ren, L.; Yang, K. Antibacterial effect of copper-bearing titanium alloy (Ti-Cu) against *Streptococcus mutans* and *Porphyromonas gingivalis*. *Sci. Rep.* **2016**, *6*, 29985. [[CrossRef](#)]

173. Fowler, L.; Engqvist, H.; Ohman-Magi, C. Effect of Copper Ion Concentration on Bacteria and Cells. *Materials* **2019**, *12*, 3798. [[CrossRef](#)] [[PubMed](#)]
174. Xu, X.; Lu, Y.; Li, S.; Guo, S.; He, M.; Luo, K.; Lin, J. Copper-modified Ti6Al4V alloy fabricated by selective laser melting with pro-angiogenic and anti-inflammatory properties for potential guided bone regeneration applications. *Mater. Sci. Eng. C Mater. Biol. Appl.* **2018**, *90*, 198–210. [[CrossRef](#)]
175. Li, M.; Ma, Z.; Zhu, Y.; Xia, H.; Yao, M.; Chu, X.; Wang, X.; Yang, K.; Yang, M.; Zhang, Y.; et al. Toward a Molecular Understanding of the Antibacterial Mechanism of Copper-Bearing Titanium Alloys against *Staphylococcus aureus*. *Adv. Healthc. Mater.* **2016**, *5*, 557–566. [[CrossRef](#)] [[PubMed](#)]
176. Baker, J.; Sitthisak, S.; Sengupta, M.; Johnson, M.; Jayaswal, R.K.; Morrissey, J.A. Copper stress induces a global stress response in *Staphylococcus aureus* and represses *sae* and *agr* expression and biofilm formation. *Appl. Environ. Microbiol.* **2010**, *76*, 150–160. [[CrossRef](#)] [[PubMed](#)]
177. Huang, Q.; Li, X.; Elkhoory, T.A.; Liu, X.; Zhang, R.; Wu, H.; Feng, Q.; Liu, Y. The Cu-containing TiO<sub>2</sub> coatings with modulatory effects on macrophage polarization and bactericidal capacity prepared by micro-arc oxidation on titanium substrates. *Colloids Surf. B Biointerfaces* **2018**, *170*, 242–250. [[CrossRef](#)]
178. Chen, L.; Wang, D.; Qiu, J.; Zhang, X.; Liu, X.; Qiao, Y.; Liu, X. Synergistic effects of immunoregulation and osteoinduction of ds-block elements on titanium surface. *Bioact. Mater.* **2021**, *6*, 191–207. [[CrossRef](#)]
179. Heidenau, F.; Mittelmeier, W.; Detsch, R.; Haenle, M.; Stenzel, F.; Ziegler, G.; Gollwitzer, H. A novel antibacterial titania coating: Metal ion toxicity and in vitro surface colonization. *J. Mater. Sci. Mater. Med.* **2005**, *16*, 883–888. [[CrossRef](#)]
180. Wolf-Brandstetter, C.; Beutner, R.; Hess, R.; Bierbaum, S.; Wagner, K.; Scharnweber, D.; Gbureck, U.; Moseke, C. Multifunctional calcium phosphate based coatings on titanium implants with integrated trace elements. *Biomed. Mater.* **2020**, *15*, 025006. [[CrossRef](#)]
181. Guo, S.; Lu, Y.; Wu, S.; Liu, L.; He, M.; Zhao, C.; Gan, Y.; Lin, J.; Luo, J.; Xu, X.; et al. Preliminary study on the corrosion resistance, antibacterial activity and cytotoxicity of selective-laser-melted Ti6Al4V-xCu alloys. *Mater. Sci. Eng. C Mater. Biol. Appl.* **2017**, *72*, 631–640. [[CrossRef](#)]
182. Macpherson, A.; Li, X.; McCormick, P.; Ren, L.; Yang, K.; Sercombe, T.B. Antibacterial Titanium Produced Using Selective Laser Melting. *JOM* **2017**, *69*, 2719–2724. [[CrossRef](#)]
183. Li, G.; Liu, S.; Zhan, D.; Liu, R.; Ren, L.; Yang, K.; Wang, J.; Wang, Q. Antibacterial Properties and Biocompatibility of SLMfabricated Medical Titanium Alloys. *Chin. J. Mater. Res.* **2019**, *33*, 117–123.
184. Liu, R.; Tang, Y.; Zeng, L.; Zhao, Y.; Ma, Z.; Sun, Z.; Xiang, L.; Ren, L.; Yang, K. In vitro and in vivo studies of anti-bacterial copper-bearing titanium alloy for dental application. *Dent. Mater.* **2018**, *34*, 1112–1126. [[CrossRef](#)] [[PubMed](#)]
185. Vilardell, A.M.; Takezawa, A.; du Plessis, A.; Takata, N.; Krakhmalev, P.; Kobashi, M.; Albu, M.; Kothleitner, G.; Yadroitsava, I.; Yadroitsev, I. Mechanical behavior of in-situ alloyed Ti6Al4V(ELI)-3 at.% Cu lattice structures manufactured by laser powder bed fusion and designed for implant applications. *J. Mech. Behav. Biomed. Mater.* **2021**, *113*. [[CrossRef](#)] [[PubMed](#)]
186. Shimabukuro, M.; Hiji, A.; Manaka, T.; Nozaki, K.; Chen, P.; Ashida, M.; Tsutsumi, Y.; Nagai, A.; Hanawa, T. Time-Transient Effects of Silver and Copper in the Porous Titanium Dioxide Layer on Antibacterial Properties. *J. Funct. Biomater.* **2020**, *11*, 44. [[CrossRef](#)]
187. Zhao, D.; Lu, Y.; Zeng, X.; Wang, Z.; Liu, S.; Wang, T. Antifouling property of micro-arc oxidation coating incorporating Cu<sub>2</sub>O nanoparticles on Ti<sub>6</sub>Al<sub>4</sub>V. *Surf. Eng.* **2017**, *33*, 796–802. [[CrossRef](#)]
188. Li, K.; Xie, Y.; Huang, L.; Ji, H.; Zheng, X. Antibacterial mechanism of plasma sprayed Ca<sub>2</sub>ZnSi<sub>2</sub>O<sub>7</sub> coating against *Escherichia coli*. *J. Mater. Sci. Mater. Med.* **2013**, *24*, 171–178. [[CrossRef](#)] [[PubMed](#)]
189. Shankar, A.H.; Prasad, A.S. Zinc and immune function: The biological basis of altered resistance to infection. *Am. J. Clin. Nutr.* **1998**, *68*, 447s–463s. [[CrossRef](#)]
190. El-Wassefy, N.A.; Reicha, F.M.; Aref, N.S. Electro-chemical deposition of nano hydroxyapatite-zinc coating on titanium metal substrate. *Int. J. Implant. Dent.* **2017**, *3*, 39. [[CrossRef](#)]
191. Shimabukuro, M.; Tsutsumi, Y.; Nozaki, K.; Chen, P.; Yamada, R.; Ashida, M.; Doi, H.; Nagai, A.; Hanawa, T. Chemical and Biological Roles of Zinc in a Porous Titanium Dioxide Layer Formed by Micro-Arc Oxidation. *Coatings* **2019**, *9*, 705. [[CrossRef](#)]
192. Liu, P.; Zhao, Y.; Yuan, Z.; Ding, H.; Hu, Y.; Yang, W.; Cai, K. Construction of Zn-incorporated multilayer films to promote osteoblasts growth and reduce bacterial adhesion. *Mater. Sci. Eng. C Mater. Biol. Appl.* **2017**, *75*, 998–1005. [[CrossRef](#)]
193. Li, Y.; Yang, Y.; Qing, Y.; Li, R.; Tang, X.; Guo, D.; Qin, Y. Enhancing ZnO-NP Antibacterial and Osteogenesis Properties in Orthopedic Applications: A Review. *Int. J. Nanomed.* **2020**, *15*, 6247–6262. [[CrossRef](#)]
194. Król, A.; Pomastowski, P.; Rafińska, K.; Railean-Plugaru, V.; Buszewski, B. Zinc oxide nanoparticles: Synthesis, antiseptic activity and toxicity mechanism. *Adv. Colloid Interface Sci.* **2017**, *249*, 37–52. [[CrossRef](#)] [[PubMed](#)]
195. Zaatreh, S.; Haffner, D.; Strauss, M.; Dauben, T.; Zamponi, C.; Mittelmeier, W.; Quandt, E.; Kreikemeyer, B.; Bader, R. Thin magnesium layer confirmed as an antibacterial and biocompatible implant coating in a co-culture model. *Mol. Med. Rep.* **2017**, *15*, 1624–1630. [[CrossRef](#)] [[PubMed](#)]
196. Subbiahdoss, G.; Sharifi, S.; Grijpma, D.W.; Laurent, S.; van der Mei, H.C.; Mahmoudi, M.; Busscher, H.J. Magnetic targeting of surface-modified superparamagnetic iron oxide nanoparticles yields antibacterial efficacy against biofilms of gentamicin-resistant staphylococci. *Acta Biomater.* **2012**, *8*, 2047–2055. [[CrossRef](#)] [[PubMed](#)]

197. Yang, T.; Qian, S.; Qiao, Y.; Liu, X. Cytocompatibility and antibacterial activity of titania nanotubes incorporated with gold nanoparticles. *Colloids Surf. B Biointerfaces* **2016**, *145*, 597–606. [[CrossRef](#)]
198. Yang, T.; Wang, D.; Liu, X. Assembled gold nanorods for the photothermal killing of bacteria. *Colloids Surf. B Biointerfaces* **2019**, *173*, 833–841. [[CrossRef](#)]
199. Yamamoto, A.; Honma, R.; Sumita, M. Cytotoxicity evaluation of 43 metal salts using murine fibroblasts and osteoblastic cells. *J. Biomed. Mater. Res.* **1998**, *39*, 331–340. [[CrossRef](#)]
200. van Hengel, I.A.J.; Tierolf, M.; Valerio, V.P.M.; Minneboo, M.; Fluit, A.C.; Fratila-Apachitei, L.E.; Apachitei, I.; Zadpoor, A.A. Self-defending additively manufactured bone implants bearing silver and copper nanoparticles. *J. Mater. Chem. B* **2020**, *8*, 1589–1602. [[CrossRef](#)]
201. Li, D.; Li, Y.; Shrestha, A.; Wang, S.; Wu, Q.; Li, L.; Guan, C.; Wang, C.; Fu, T.; Liu, W.; et al. Effects of Programmed Local Delivery from a Micro/Nano-Hierarchical Surface on Titanium Implant on Infection Clearance and Osteogenic Induction in an Infected Bone Defect. *Adv. Healthc. Mater.* **2019**, *8*. [[CrossRef](#)]
202. Kirmanidou, Y.; Sidira, M.; Drosou, M.E.; Bennani, V.; Bakopoulou, A.; Tsouknidas, A.; Michailidis, N.; Michalakis, K. New Ti-Alloys and Surface Modifications to Improve the Mechanical Properties and the Biological Response to Orthopedic and Dental Implants: A Review. *Biomed. Res. Int* **2016**, *2016*, 2908570. [[CrossRef](#)] [[PubMed](#)]
203. Wang, L.; Xie, L.; Shen, P.; Fan, Q.; Wang, W.; Wang, K.; Lu, W.; Hua, L.; Zhang, L.-C. Surface microstructure and mechanical properties of Ti-6Al-4V/Ag nanocomposite prepared by FSP. *Mater. Charact.* **2019**, *153*, 175–183. [[CrossRef](#)]
204. Attarilar, S.; Djavanroodi, F.; Ebrahimi, M.; Al-Fadhalah, K.J.; Wang, L.; Mozafari, M. Hierarchical Microstructure Tailoring of Pure Titanium for Enhancing Cellular Response at Tissue-Implant Interface. *J. Biomed. Nanotechnol.* **2021**, *17*, 115–130. [[CrossRef](#)] [[PubMed](#)]